

Structural Dynamics of Aqueous Salt Solutions

H. J. Bakker

Chem. Rev., **2008**, 108 (4), 1456-1473 • DOI: 10.1021/cr0206622

Downloaded from <http://pubs.acs.org> on December 24, 2008

More About This Article

Additional resources and features associated with this article are available within the HTML version:

- Supporting Information
- Links to the 2 articles that cite this article, as of the time of this article download
- Access to high resolution figures
- Links to articles and content related to this article
- Copyright permission to reproduce figures and/or text from this article

[View the Full Text HTML](#)



ACS Publications
High quality. High impact.

Structural Dynamics of Aqueous Salt Solutions

H. J. Bakker

FOM Institute for Atomic and Molecular Physics, Kruislaan 407, 1098 SJ Amsterdam, The Netherlands

Received November 3, 2005, Received Revised September 26, 2007

Contents

1. General Introduction	1456
2. Structural Dynamics of Ionic Hydrations Shells	1457
2.1. Introduction	1457
2.2. Nuclear Magnetic Resonance	1457
2.2.1. Translational Dynamics	1457
2.2.2. Orientational Dynamics	1458
2.3. Depolarized Rayleigh Scattering	1459
2.4. Transient Vibrational Absorption Spectroscopy	1459
2.4.1. Translational Dynamics	1459
2.4.2. Orientational Dynamics	1461
2.5. Molecular Dynamics Simulations	1462
2.6. Discussion	1463
3. Energy Dynamics of Ionic Hydration Shells	1464
3.1. Introduction	1464
3.2. Vibrational Relaxation of Anionic Hydration Shells	1464
3.3. Effect of Concentration on the Energy Dynamics of the Anionic Hydration Shell	1465
3.4. Effect of Cations on the Energy Dynamics of the Anionic Solvation Shell	1466
3.5. Temperature Dependence of the Energy Dynamics of the Anionic Solvation Shell	1467
4. Structural Dynamics of Water Outside the First Ionic Hydration Shell	1467
4.1. Introduction	1467
4.2. Low-Frequency Raman Scattering and Optical Kerr Effect	1468
4.3. Dielectric Relaxation and Low-Frequency Infrared Spectroscopy	1468
4.4. Transient Vibrational Absorption Spectroscopy	1469
4.5. Molecular Dynamics Simulations	1471
4.6. Discussion and Concluding Remarks	1471
5. Acknowledgments	1472
6. References	1472



Huib Johan Bakker was born on March 2, 1965, in Haarlem, The Netherlands. He did his undergraduate studies in chemistry at the Vrije Universiteit in Amsterdam and received his diploma in physical chemistry in 1987. During his Ph.D. studies in the group of Prof. dr. Ad Legendijk, at the FOM Institute for Atomic and Molecular Physics (AMOLF), he studied the vibrational dynamics of small organic molecules with picosecond mid-infrared laser pulses. In 1991, he received his Ph.D. degree “cum laude”. From 1991–1994 he worked as a post-doc in the group of Prof. dr. Heinz Kurz at the Institute of Semiconductor Electronics at the Technical University of Aachen, Germany. In this time period he studied the dynamics of phonons, plasmons, and polaritons in ferroelectrics and semiconductor heterostructures. In 1995 he became a group leader at AMOLF, heading the group “Ultrafast Spectroscopy”. The research work of the group includes the spectroscopic study of the structure and ultrafast dynamics of water interacting with ions and (bio)molecular systems and the study of the mechanism of proton transfer in aqueous media. In 2001 he became a full professor of Physical Chemistry at the University of Amsterdam, The Netherlands, and in 2003 he became department head “Ultrafast Molecular Dynamics” at AMOLF. In 2004, he received the Gold Medal of the Royal Netherlands Chemical Society for his work on the ultrafast dynamics of aqueous systems.

The addition of ions to water has a dramatic effect on the structure of the liquid. Conventional infrared absorption and Raman spectroscopic studies show that the addition of salt to water leads to a severe disruption of the hydrogen-bonded structure of the liquid and to the formation of solvation shells.^{1–3} In the past few decades, the structural properties of ionic hydration shells have been studied with a variety of experimental and theoretical techniques including X-ray scattering, neutron diffraction, NMR, Rayleigh, Brillouin scattering, and molecular dynamics simulations. At present for most ions, the coordination numbers of the hydration shells are known, and the mean distances between the ions and the water molecules in the first and the second hydration shells have been determined. A nice overview of these results can be found in ref 4.

The effect of ions on the structure of water is probably not restricted to the formation of first and second hydration shells. It is generally assumed that ions also have a long-

1. General Introduction

Saltwater is the most ubiquitous liquid on earth: two-thirds of the surface of the earth is covered by this liquid. It may, thus, not be a coincidence that saltwater also forms the main constituent of most living organisms. About 70% of the human body is formed by water with dissolved salts, and human blood can be replaced partly by so-called “physiological salt”, which is a solution of 8 (g of NaCl)/(L of water).

* Tel.: 31-20-6081234. Fax: 31-20-6684106. E-mail: bakker@amolf.nl.

range effect on the hydrogen-bond structure of liquid water, either enhancing or weakening this structure. This idea was first introduced in 1934 by Cox and Wolfenden.⁵ Some ions would serve as a nucleation seed for a more icelike structure of the liquid (“structure makers”), while other ions would rather destroy the tetrahedral hydrogen-bond structure (“structure breakers”). Small and multiply charged ions are believed to induce a strengthening of the hydrogen-bond structure and are denoted as structure makers. Large, monovalent ions are rather believed to lead to a weakening of the hydrogen-bond network and are, thus, denoted as structure breakers. The evidence for the concept of structure making and breaking mainly stems from the measurement of the viscosity⁶ and the ion mobilities of aqueous salt solutions.⁷

The *dynamics* of aqueous salt solutions have also been studied with experimental techniques like NMR, low-frequency Raman scattering, and dielectric relaxation spectroscopy. An often-encountered problem in these studies is that the intrinsic measuring times are long (nanosecond to microsecond time range) compared to the exchange time of water between the hydration shells and the bulk (picosecond). An additional problem is that it is difficult to distinguish the dynamics of the solvation shells from the bulk liquid. As a result, at present most of the dynamical information of ionic hydration shells does not come from experimental studies but stems from molecular dynamics simulations.^{8–24}

In the past decade, it has become possible to study the dynamics of bulk liquid water and hydration shells on the subpicosecond time scale with ultrafast spectroscopic techniques. In many of these studies, light pulses are used that are resonant with a dissolved probe molecule or ion.^{25–31} The dynamics of the probe molecule/ion depends on the interactions between the ions and water and, thus, may provide information on the effects of the probe molecule/ion on the properties of water. However, the measured response is often dominated by the internal properties of the dissolved probe molecule/ion. The ultrafast dynamics of aqueous systems have also been studied by probing the vibrational resonances of the (solvating) water molecules with ~100 fs (10^{-13} s) midinfrared laser pulses.^{32–44} The advantage of this technique applied to aqueous salt solutions is that the dynamics of the water molecules are probed directly and not via the response of a dissolved probe molecule/ion.

The molecular scale properties of ionic hydration shells have been reviewed before in an excellent manner by Ohtaki and Radnai⁴ in this journal in 1993. Since that time, there have been interesting developments in the fields of molecular dynamics simulations and ultrafast spectroscopy that have led to new information on ionic hydration shells, in particular on their dynamics. In this review, the dynamics of water molecules near ions will be discussed in the light of the recent findings, and in perspective with previous work on the structure and dynamics of ionic hydration shells. This review is organized in the following way. In section 2, the results on the structural dynamics of the hydration shells of ions are presented and discussed. In section 3, the vibrational relaxation dynamics of these hydration shells are described, and finally, in section 4, the effects of ions on the structure and dynamics of aqueous salt solutions *outside* the hydration shells are treated. These latter results shed new light on the long-range effects of ions on the dynamics and hydrogen-bond structure of liquid water, in particular on the concept of structure making and breaking.

2. Structural Dynamics of Ionic Hydrations Shells

2.1. Introduction

Hydration shells of ions are dynamical structures showing (deformation) vibrations and rotations. In addition, water molecules are continuously being exchanged between the shell and the surrounding bulk liquid. The dynamics of ionic hydration shells have been studied with NMR, depolarized Rayleigh scattering, transient vibrational absorption spectroscopy, and molecular dynamics simulations. Here, we give an overview and discussion of the results obtained.

2.2. Nuclear Magnetic Resonance

Nuclear magnetic resonance (NMR) spectroscopy is a powerful technique to study the structure and dynamics of water molecules in aqueous salt solutions. For specific ions that strongly bind water molecules, the exchange frequency between the solvation shell and the bulk is lower than the frequency splitting of the spin resonances associated with water in the solvation shell and water in the bulk. As a result, the water molecules in the solvation shell give rise to a well-separated peak in the NMR spectrum. This is, for instance, the case for ions like Be^{2+} , Mg^{2+} , and Al^{3+} .⁴⁵ In these cases, the coordination number of the solvation shell can easily be determined from the integral of the peak in the NMR spectrum. For most other ions, the exchange between bulk and solvation shell is too fast to resolve a separate peak in the NMR spectrum. In this motional narrowing case, the water molecules in the bulk and the solvation shell give rise to a single peak of which the position gives information on the coordination number. In addition to structural information, NMR can also be used to study the dynamics of the solvating water molecules.

2.2.1. Translational Dynamics

Information on the translational mobility of water molecules can be obtained using NMR spin-echo techniques in a steady magnetic field gradient. In a magnetic field gradient, the spin-echo amplitude is given by⁴⁶

$$S(2\tau) = S(0) e^{-2\tau/T_2} e^{-2\gamma^2 G^2 D \tau^3/3} \quad (1)$$

with τ the time between the two radio frequency pulses, T_2 the transverse relaxation time, γ the gyromagnetic ratio, G the magnetic field gradient, and D the self-diffusion coefficient of the water molecules. The amplitude of the spin echo as a function of time τ gives information on the self-diffusivity and, thus, on the translational dynamics of the water molecules.

The dependence of D on the concentration of dissolved salt can be expressed in the following way,⁴⁷

$$\frac{D^0}{D(c)} = 1 + B_D c + \dots \quad (2)$$

where D^0 is the self-diffusion coefficient of water in the absence of salt. For dissolved salts with tightly bound solvation shells, B_D is positive, which implies that D is smaller than for pure water. For dissolved salts with weakly bound solvation shells, B_D is negative and D will be larger than for pure water. A problem in using this approach that the contribution to the mobility of water molecules solvating the positive ions cannot be distinguished from the contribu-

tion of water molecules solvating the negative ions. To solve this issue, it is assumed that $B_D(\text{K}^+) = B_D(\text{Cl}^-)$. Using this assumption, it is possible to obtain B_D^\pm coefficients for water in the solvation shells of individual ions. If it is further assumed that the observed diffusivity is an average of the diffusivities of the solvation shells and the (unchanged) diffusivity of bulk water, the value of D^\pm can be related to B_D^\pm with the following equation,

$$D^0/D^\pm = B_D^\pm \frac{55.5}{n_c^\pm} + 1 \quad (3)$$

where 55.5 is the molar concentration of pure water and n_c is the coordination number of the solvation shell. The last equation shows that, with increasing B_D^\pm , the diffusivity and, thus, the translational mobility decreases.

The self-diffusion constants determined by NMR can be used to determine the residence time τ of a water molecule in the hydration shell by using the Einstein–Smoluchovski relation ($\tau = l^2/2D$, with l being the distance over which the molecule moves). Here, we use the version of this equation in one dimension being the radial direction to the ion. Using for l the average oxygen–oxygen distance in water of 2.8×10^{-10} m and the values of D determined from the spin-echo measurements,⁴⁷ we obtain $\tau = 15$ ps for Cl^- , 10 ps for Br^- , and 5 ps for I^- . For positive ions, the residence times are longer: $\tau = 39$ ps for Li^+ , $\tau = 27$ ps for Na^+ , and $\tau = 15$ ps for K^+ (by definition the same as for Cl^-). The longest residence times are found for doubly valent positive ions: $\tau = 90$ ps for Mg^{2+} and $\tau = 60$ ps for Ca^{2+} .

2.2.2. Orientational Dynamics

NMR spectroscopy can also be used to get information on the orientational dynamics of the hydration shell. The magnetic field of the proton spin adds to the magnetic field experienced by other nearby protons. As a result, the relative motions of the molecules lead to fluctuations in the local magnetic fields. These fluctuations enable transitions between spin states and, thus, lead to relaxation. The longitudinal spin relaxation time constant T_1 can be written as⁴⁸

$$\frac{1}{T_1} = CE_i^2 f(\tau_c) \quad (4)$$

with C a constant, E_i the interaction energy of the process responsible for the relaxation (for instance nuclear dipole–nuclear dipole interaction), and $f(\tau_c)$ a function of the correlation time constant τ_c . In the motional narrowing limit, $f(\tau_c)$ is proportional to τ_c . Note that this means that slower fluctuations (long τ_c) lead to faster relaxation (short T_1). The value of τ_c is determined by the fluctuations in the distance and relative orientation of the interacting nuclear dipoles. The longitudinal spin relaxation time constant T_1 measured in NMR can, thus, be used to determine the time constants of the relative motions of the molecules.

The observed longitudinal spin relaxation can result both from interactions between nuclear spins located on the same molecule (intramolecular) and from interactions between nuclear spins located on different molecules (intermolecular). The intramolecular contribution to the longitudinal relaxation requires a modulation of the interaction between the spins located on the same molecule. Such a modulation results from the molecular reorientation. The intermolecular contribution to T_1 requires the relative motion of different

molecules, which can thus be associated with the translational molecular mobility. Hence, the observed spin relaxation is a sum of two contributions:⁴⁸

$$\frac{1}{T_1(c)} = \frac{1}{T_{1,\text{rot}}(c)} + \frac{1}{T_{1,\text{trans}}(c)} \quad (5)$$

For some solvents like DMSO, the rotational and the translation contributions to the longitudinal relaxation can be distinguished.⁴⁸ For these solvents, the value of $T_{1,\text{trans}}(c)$ can be determined using the value of $T_{1,\text{trans}}(0)$ of the pure solvent and the concentration-dependent self-diffusion coefficients that are determined using magnetic-field gradient spin-echo techniques:

$$\frac{1}{T_{1,\text{trans}}(c)} = \frac{1}{T_{1,\text{trans}}(0)} \frac{D(c=0)}{D(c)} \quad (6)$$

The value of $T_{1,\text{rot}}(0)$ (and, thus, of $T_{1,\text{trans}}(0)$) can be determined from measurements on the pure solvent in isotopic dilution.⁴⁸

For water, it is not possible to determine $T_{1,\text{rot}}(0)$ and $T_{1,\text{trans}}(0)$ separately, because for this solvent, isotopic dilution leads to the formation of HDO molecules. Hence, for water, isotopic dilution affects both the rotational and the translational contribution to the longitudinal spin relaxation. Therefore, for water, it has been assumed that the two relaxation contributions show the same dependence on the nature of the ions and the concentration. Hence, τ_{or} is proportional to τ_c . Following Hertz,⁴⁷ the dependence of T_1 on the concentration of dissolved salt can be expressed in the following way:

$$\frac{T_1(0)}{T_1(c)} = 1 + B_{\text{rot}}c + \dots \quad (7)$$

For salts that have tightly bound solvation shells, B_{rot} is positive, meaning that the spin relaxation time is observed to be shorter; for salts that have weakly bound solvation shells, B_{rot} is negative and T_1 is longer. As with the change in diffusivity, it can be assumed that the observed change in T_1 is the sum of the contributions of the positive and negative ions and that $B_{\text{rot}}(\text{K}^+) = B_{\text{rot}}(\text{Cl}^-)$. If it is further assumed that the observed T_1 is a weighted average of T_1 of the spins in the solvation shells and of the unchanged T_1 of the bulk, and using $1/T_1 \approx \tau_{\text{or}}$, the coefficients B_{rot}^\pm can be directly related to the correlation time constant τ_{or}^\pm for molecular reorientation in the shell,

$$\tau_{\text{or}}^\pm/\tau_{\text{or}}^0 = B_{\text{rot}}^\pm \frac{55.5}{n_c^\pm} + 1 \quad (8)$$

where 55.5 is the molar concentration of pure water and n_c is the coordination number of the solvation shell. The last equation shows that, with increasing B_{rot}^\pm , the correlation time constant increases. Hence, for rigid solvation shells with slow orientational dynamics (large τ_{or}^\pm and B_{rot}^\pm), the longitudinal relaxation time T_1 is short.

The rotational correlation time constant τ_{or} is defined as the decay time of the second-order correlation function $C_2(t) = \langle P_2(\mathbf{e}(t) \cdot \mathbf{e}(0)) \rangle = e^{-t/\tau_{\text{or}}}$, where $P_2(x)$ is the second Legendre polynomial in x . For the rotational correlation time constant of pure liquid water (τ_{or}^0), a value of 2.5 ps at 300

K has been found, both with NMR^{49,50} and with transient vibrational spectroscopy.⁵¹ From the measured changes in the longitudinal relaxation times, it was deduced that the rotational dynamics of water in the hydration shells of multivalent ions like Mg^{2+} and Ca^{2+} are slower by a factor of 5 than in bulk water. In contrast, the rotational dynamics of water in the hydration shells of large monovalent ions like Cs^+ and I^- were found to be faster than those in bulk water.

2.3. Depolarized Rayleigh Scattering

The orientational dynamics of ionic hydration shells have also been studied with depolarized Rayleigh scattering. The line width measured in this technique is believed to be mainly determined by the orientational dynamics of the water molecules in the hydration shells, as the depolarised light scattering from pure water is very weak.⁵² For a solution of LiCl in H_2O , the reorientation time constant is observed to increase from 7 ps at low concentrations to 18 ps at high concentrations (36 mol % solution).⁵² The slow orientational dynamics are interpreted to be mainly due to water molecules solvating the Li^+ ions. These ions are, thus, found in these measurements to show rotational dynamics that are 3–6 times slower than in bulk water.

2.4. Transient Vibrational Absorption Spectroscopy

Recently, it has become possible to study the translational and orientational motions of water molecules interacting with ions with femtosecond transient vibrational spectroscopy.^{53–61} In this technique, a molecular vibration of water is excited by an intense infrared light pulse, thereby transferring a significant fraction of the molecules to the first excited state ($\nu = 1$) of the vibration. In the case of excitation of an O–H stretch vibration, the required midinfrared pulse has a central wavelength of $\sim 3 \mu\text{m}$ ($\approx 3300 \text{ cm}^{-1}$); in the case of excitation of an O–D stretch vibration, the required midinfrared pulse has a central wavelength of $\sim 4 \mu\text{m}$ ($\approx 2500 \text{ cm}^{-1}$).

The decay of the excitation is measured with a second pulse (probe) that is resonant with either the fundamental $0 \rightarrow 1$ transition or with the $1 \rightarrow 2$ excited-state absorption. For the O–H stretch vibrations of water, the latter absorption is anharmonically red-shifted by $\sim 250 \text{ cm}^{-1}$. For the O–D stretch vibration, the anharmonic shift is $\sim 180 \text{ cm}^{-1}$. If the probe is resonant with the fundamental $0 \rightarrow 1$ transition, the excitation by the pump leads to a transient transmission increase, because less molecules are in the $\nu = 0$ state, and because of $1 \rightarrow 0$ stimulated emission out of the $\nu = 1$ state. The excitation to $\nu = 1$ also leads to $1 \rightarrow 2$ excited-state absorption and, thus, to a decrease in the probe transmission at frequencies that are resonant with this transition.

In the reported transient vibrational absorption spectroscopic studies of aqueous salt solutions,^{53–61} the dynamics of a large range of salts has been studied, including KF , LiCl , LiBr , LiI , NaCl , NaBr , NaI , MgCl_2 , MgBr_2 , MgI_2 , NaClO_4 , and $\text{Mg}(\text{ClO}_4)_2$. The salt solutions have been studied over a wide range of concentrations, ranging from 0.5 to 10 M. In all studies, a low-concentration solution of HDO in D_2O is used as a solvent, because for O–H concentrations $> 1 \text{ M}$, the vibrational dynamics are affected by resonant energy transfer among the O–H stretch vibrations.³⁷ In a solution of 0.1 M HDO in D_2O , the O–H vibrations are sufficiently

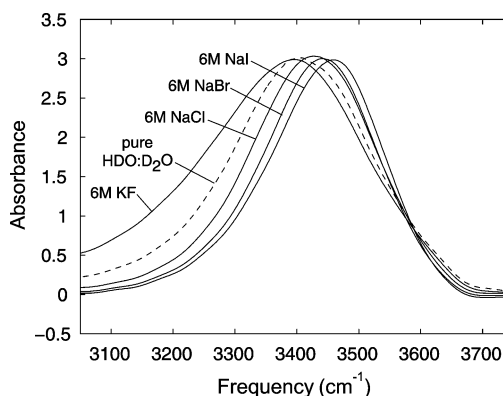


Figure 1. Absorption spectra of a solution of 0.5 M HDO in D_2O and of solutions of 0.5 M HDO and 6 M KF , NaCl , NaBr , or NaI in D_2O . Reprinted with permission from ref 58. Copyright 2002 Elsevier.

isolated to prevent the dynamics to be influenced by this process. Clearly, the solvent HDO/ D_2O is not the same as pure H_2O . However, it can be expected that this will not lead to qualitatively different results because D_2O and H_2O show quite similar hydrogen-bond structures and interactions. The pump and probe pulses used in these experiments have a duration of $\sim 100 \text{ fs}$.

2.4.1. Translational Dynamics

The dissolution of halogenic anions in liquid water has been found to lead to the formation of hydrogen bonds between the ion and the solvating water molecule.^{2,62} These newly formed $\text{O}-\text{H}\cdots\text{X}^-$ ($\text{X}^- = \text{Cl}^-$, Br^-) hydrogen bonds are directional in character,^{2,62} which means that the O–H bond and the $\text{O}\cdots\text{X}^-$ hydrogen-bond coordinates are colinear.

In Figure 1, the linear absorption spectra of the O–H stretch vibration of HDO molecules of an aqueous solution consisting of HDO (0.5 M) in D_2O and 6 M of KF , NaCl , NaBr , or NaI are shown. Within the halogenic series (F^- , Cl^- , Br^- , I^-), the absorption spectrum of the O–H stretch vibration is observed to shift to higher frequencies. The shift to higher frequencies indicates that the average hydrogen-bond becomes longer and weaker.^{63–65}

The O–H stretch frequency depends strongly on the length of the hydrogen bond that involves the hydrogen atom of the O–H group.^{63–65} Fluctuations in the length of the hydrogen bonds will, thus, lead to fluctuations of the O–H stretch vibration frequencies. This is the case for both the $\text{O}-\text{H}\cdots\text{O}$ hydrogen bonds to oxygen atoms of other water molecules and the directional $\text{O}-\text{H}\cdots\text{X}^-$ hydrogen bonds to halogenic anions X^- .^{2,62}

As will be shown in the next section, the lifetime of the O–H stretch vibrations of water in the solvation shells of the halogenic anions Cl^- , Br^- , and I^- is longer by a factor of 3–5 than the vibrational lifetime of the bulk. This property can be employed to distinguish the hydrogen-bond dynamics of these water molecules from the dynamics of bulk water molecules. A pump pulse with a frequency near 3400 cm^{-1} will excite all water molecules, including bulk water molecules and the water molecules in the hydration shells of the cations and the anions. The vibrational excitations of water molecules in the bulk and in the solvation shells of the cations decay with a time constant of $\sim 800 \text{ fs}$,⁵³ whereas the excitations in the first hydration shells of the Cl^- , Br^- , or I^- ions decay on a much larger time scale. Hence, after a

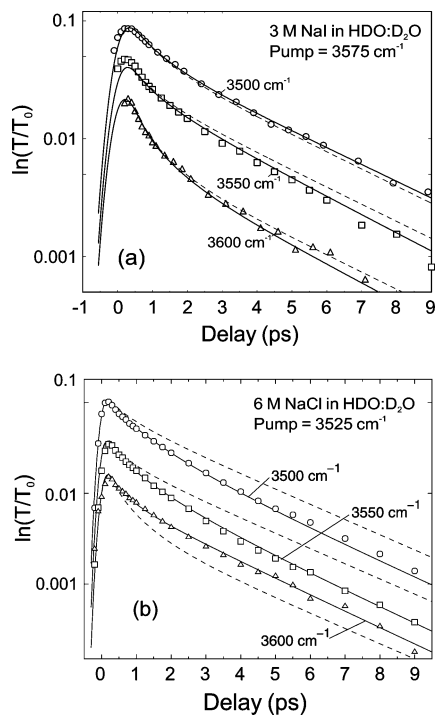


Figure 2. Pump–probe transients measured for aqueous solutions of 3 M NaI in HDO/D₂O and 6 M NaCl in HDO/D₂O. The transients are offset with respect to each other and are plotted on a logarithmic scale to clarify the presence of two absorption components and the differences in time constants. The solid curves are calculated with a Brownian oscillator model, using a τ_c of 18 ps for the modulation of the O–H \cdots I[−] hydrogen bond and a τ_c of 12 ps for the modulation of the O–H \cdots Cl[−] hydrogen bond. The dashed curves are calculated with the same model using $\tau_c = \infty$. (a) Reprinted with permission from ref 53. Copyright 2001 AAAS. (b) Reprinted with permission from ref 54. Copyright 2001 American Institute of Physics.

few picoseconds, the signals observed in the transient pump–probe experiments represent *only* the response of water molecules that form O–H \cdots X[−] hydrogen bonds (X[−] = Cl[−], Br[−], I[−]). As a result, the translational and orientational dynamics of these water molecules can be selectively probed by monitoring the signals measured at delays > 3 ps.

In Figure 2, pump–probe transients are shown that are measured for solutions of 3 M NaI and 6 M NaCl using different probe frequencies. The transients show a fast relaxation component corresponding to the vibrational relaxation of O–H groups of bulk water and of water molecules solvating cations and a slow component corresponding to the vibrational relaxation of O–H groups that are hydrogen bonded to the anions. The time constant of the slow relaxation component shows a small but significant dependence on the probe frequency. The time constant of the slow component is observed to increase with increasing frequency difference between pump and probe. This frequency dependence of the decay time results from the spectral diffusion of the excitation frequency, which, in turn, results from the fluctuations in the length of the O–H \cdots X[−] hydrogen bond between the solvating HDO molecule and the X[−] halogenic anion. Because of this spectral diffusion process, excited molecules diffuse (spectrally) away from the excitation frequency, which leads to a faster decay at probe frequencies close to the pump frequency and a slower decay at probe frequencies that significantly differ from the pump frequency.

Table 1. Central Frequency ω_0 , Width $\Delta\omega$, Vibrational Lifetime T_1 , and Spectral Diffusion Time τ_c of the O–H Stretch Vibration of Different Hydrogen-Bonded O–H Groups, Obtained by Fitting the Data Using a Two-Component Brownian Oscillator Model^a

	ω_0 (cm ^{−1})	$\Delta\omega$ (cm ^{−1})	T_1 (ps)	τ_c (ps)
O–H \cdots O	3420 ± 10	280 ± 20	0.8 ± 0.1	0.5 ± 0.2
O–H \cdots Cl [−]	3440 ± 15	160 ± 15	2.6 ± 0.2	12 ± 3
O–H \cdots Br [−]	3470 ± 15	130 ± 15	3.0 ± 0.2	25 ± 5
O–H \cdots I [−]	3490 ± 15	105 ± 15	3.7 ± 0.3	18 ± 5

^a The Values are Obtained for 6 M Solutions of NaCl, NaBr, and NaI Dissolved in HDO/D₂O. For All Solutions, the Same Set of Values for the O–H \cdots O Component Was Used.

In order to determine the correlation time constant τ_c of the spectral diffusion, the data are described with a Brownian oscillator model. Recently, it was shown that this model provides a good description of the spectral dynamics of the O–H stretching mode of HDO dissolved in D₂O.³⁶ In the Brownian oscillator model, the frequency fluctuations of a high-frequency coordinate are directly related to the motion in a low-frequency coordinate, i.e., the transition frequency is defined by the value of this low-frequency coordinate. The motion in the low-frequency coordinate is assumed to be governed by a harmonic potential and by stochastic interactions with a surrounding bath (Brownian oscillator). In the present case, the low-frequency coordinate is the hydrogen-bond length, i.e., the distance between the oxygen atoms for the O–H \cdots O hydrogen-bonded systems and the distance between the oxygen atom and the X[−] halogenic anion for the O–H \cdots X[−] hydrogen-bonded systems. The motion along this hydrogen bond represents the translational motion of the solvating water molecules with respect to the ion.

In isolated hydrogen-bonded systems, the interactions with the bath are weak and the low-frequency oscillation will be underdamped. However, for liquid-phase aqueous systems, the interactions with the bath are strong, and the spectral response of the high-frequency oscillator can often be described assuming diffusive, overdamped motion in the low-frequency coordinate. For pure HDO/D₂O, such a description was successful in describing the spectral response at delays > 200 fs.^{35,36} However, at shorter delays, evidence was found that the hydrogen-bond mode is, in fact, not overdamped and shows some residual oscillatory behavior.^{40,66,67} In the modeling of the data obtained for aqueous solutions, the hydrogen-bond modes are assumed to be overdamped.^{53,54}

All transients are fitted with two Brownian oscillators that represent the O–H \cdots O and O–H \cdots X[−] components, respectively. The parameters of these Brownian oscillators are shown in Table 1. The results of the calculations are shown in Figure 2 by the solid curves. For all solutions, the same set of parameters for the O–H \cdots O component is obtained. The spectral diffusion of this component has a time constant τ_c of 500 fs, which corresponds to the results of earlier studies on the hydrogen-bond dynamics of liquid water.^{35,36} In more recent studies of pure liquid water performed with a better time resolution, it was found that the hydrogen-bond dynamics of liquid water, in fact, consists of two components of similar amplitude with time constants of \sim 100 fs and \sim 1 ps.⁴⁰ Hence, the value of τ_c of 500 fs likely represents a weighted average of the two components of the hydrogen-bond dynamics of the bulk liquid.

The time constants τ_c represent the correlation time constants of the hydrogen-bond fluctuations that keep the

O–H···X[−] hydrogen bond intact. As soon as the fluctuations would lead to breaking of this bond and, more importantly, to the formation of a new hydrogen bond to an oxygen atom of a neighboring water molecule, the excitation of the O–H stretch vibration would rapidly relax and the O–H oscillator would vanish from the signal.⁷⁰ Therefore, the time constants τ_c do not include fluctuations that lead to the transformation of the O–H···X[−] hydrogen bond into an O–H···O hydrogen bond.

The time constants presented in Table 1 are determined at quite high concentrations of ions. For a solution of 6 M NaCl, approximately $6 \times \sim 5 = \sim 30$ M of the ~ 110 M O–H groups will form O–H···Cl[−] hydrogen bonds, while the remaining ~ 80 M O–H groups will form O–H···O hydrogen bonds. Clearly, the latter ~ 80 M are not bulk water O–H groups: the majority of these O–H groups will belong to water molecules in the first hydration shells of the Na⁺ and Cl[−] ions. The precise location of the O–H···O oscillator appears to have very little effect on the energy dynamics and the translational hydrogen-bond dynamics of the O–H group. The values found for T_1 and τ_c at high salt concentrations are very similar to the values of these parameters of pure liquid HDO/D₂O.^{34–36} This may seem surprising because the interactions with the oxygen atom of the O–H group will be very different: in bulk water, the oxygen atom will accept hydrogen bonds from neighboring water molecules, whereas in a concentrated NaX solution, a large fraction of the oxygen atoms will be located near a Na⁺ ion. It thus appears that the interactions with the oxygen atom of the O–H group have very little effect on the energy and hydrogen-bond dynamics of the O–H group. Only the spectral width of the O–H···O component appears to be somewhat larger (280 cm^{−1}) than that for bulk liquid water (260 cm^{−1}), which can be explained from the large heterogeneity of highly concentrated salt solutions.

The central frequency of the O–H···X[−] component increases in the halogenic series Cl[−], Br[−], and I[−], reflecting a decrease of the strength of the hydrogen-bond interaction between the solvating HDO molecule and the anion. This increase of the central frequency agrees with the observations in the linear absorption spectra of Figure 1 and with the results of a study in which the change in O–D stretch frequency due to salt addition was measured using a double-difference spectroscopic technique.⁶² After multiplying by 1.36 to convert O–D into O–H stretch frequencies,⁶⁸ the central absorption frequencies found in these studies are 3441 cm^{−1} (O–H···Cl[−]), 3476 cm^{−1} (O–H···Br[−]), and 3495 cm^{−1} (O–H···I[−]).

The widths of the absorption components can be translated into widths of the distributions of hydrogen-bond lengths, as the O–H stretch vibrational frequency and the length of the hydrogen bond are correlated.^{64,65} For the O–H···Cl[−], O–H···Br[−], and O–H···I[−] hydrogen bonds, the widths of the length distributions are 20 ± 5 pm ($=10^{-12}$ m), 21 ± 5 pm, and 12 ± 4 pm, respectively (the mean lengths of these hydrogen bonds are 320, 340, and 360 pm, respectively). These widths are relatively small compared to the width of 36 ± 2 pm of the distribution of O–H···O hydrogen-bond lengths of HDO/D₂O. This finding implies that the O–H···X[−] hydrogen bonds have a relatively well-defined length. It should be noted that the widths determined from the absorption bands of the O–H···X[−] component represent, in fact, upper limits of the true widths; the widths of the length distributions may be even narrower, because line-broadening

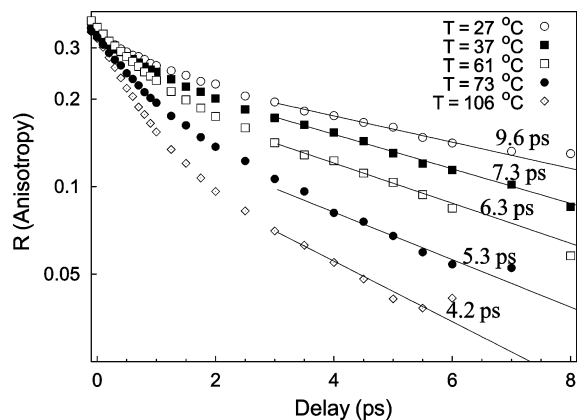


Figure 3. Anisotropy parameter R as a function of delay τ for a solution of 3 M NaCl in HDO/D₂O at five different temperatures. The pump frequency is 3450 cm^{−1}, and the probe frequency is 3200 cm^{−1}. Also shown are exponential fits to the transients in the delay-time range from 3 to 8 ps (solid curves). Reprinted with permission from ref 56 (<http://link.aps.org/abstract/PRL/v88/p77601>). Copyright 2002 American Physical Society.

mechanisms other than the spread in hydrogen-bond lengths may contribute to the width of the absorption band.

2.4.2. Orientational Dynamics

The rate of molecular reorientation of the water molecules can be studied by measuring the time dependence of the anisotropy of the excitation of the O–H stretch vibration. The excitation is initially anisotropic following a $\cos^2(\theta)$ distribution (θ being the angle between the O–H transition dipole and the pump polarization), because O–H groups have the largest chance for excitation when they are oriented parallel to the pump polarization ($\theta = 0$). As a result, the absorption change $\Delta\alpha_{\parallel}$ for the case where the probe polarization is parallel to the pump polarization will be larger than the absorption change $\Delta\alpha_{\perp}$ for the case where the probe polarization is perpendicular to the pump polarization. From $\Delta\alpha_{\parallel}$ and $\Delta\alpha_{\perp}$, the rotational anisotropy⁶⁹ can be calculated:

$$R = \frac{\Delta\alpha_{\parallel} - \Delta\alpha_{\perp}}{\Delta\alpha_{\parallel} + 2\Delta\alpha_{\perp}} \quad (9)$$

It can be shown that $R(t) = \langle P_2(\mathbf{e}(t) \cdot \mathbf{e}(0)) \rangle = e^{-t/\tau_{or}}$, where \mathbf{e} denotes the direction of the transition dipole moment of the molecular (O–H) vibration.⁵¹ As a result, the reorientation time τ_{or} obtained from the dynamics of R can be directly compared with the results from NMR. The denominator of eq 9 represents the isotropic signal that is not affected by the reorientation.⁶⁹ Hence, isotropic effects like vibrational relaxation and spectral diffusion are divided out in the expression for R , so that the delay dependence of R only represents the orientational dynamics of the water molecules.

In Figure 3, the anisotropy parameter R is presented as a function of delay for a solution of 3 M NaCl in HDO/D₂O at different temperatures. All signals show an overall nonexponential decay but become close to a single exponential for delays > 3 ps. After this delay time, the signals only represent the orientational dynamics of the HDO molecules in the first hydration shell of the Cl[−] ion, as a result of the difference in vibrational lifetime of the O–H···O and the O–H···Cl[−] hydrogen-bonded systems. Also shown in Figure 3 are fits to the data in the delay-time window from 3 to 8 ps. At 27 °C, the time constant τ_{or} of the orientational relaxation of these HDO molecules is 9.6

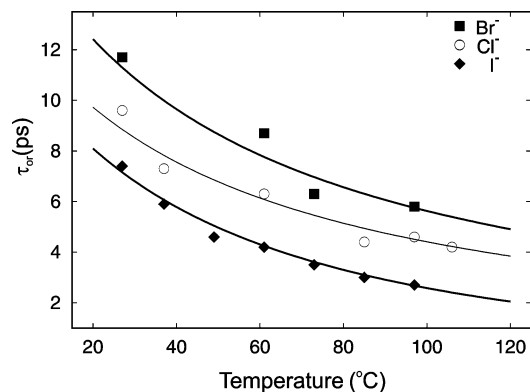


Figure 4. Time constants τ_{or} of the hydration shells of Cl^- , Br^- , and I^- as a function of temperature. The solid curves represent fits of the data using eq 10. Reprinted with permission from ref 56 (<http://link.aps.org/abstract/PRL/v88/p77601>). Copyright 2002 American Physical Society.

± 0.6 ps, which is long in comparison with the value of τ_{or} of 2.6 ps of HDO molecules in a solution of HDO in D_2O .⁵¹ With increasing temperature, the orientational relaxation becomes faster: τ_{or} decreases to 4.2 ± 0.4 ps at 106 °C.

In a recent molecular dynamics simulation on the reorientation of water molecules solvating Cl^- ,⁷⁰ it was pointed out that the reorientation time constants τ_{or} of the hydration shells represent the reorientation of the intact hydrogen-bonded $\text{O}-\text{H}\cdots\text{X}^-$ systems. As soon as this hydrogen bond breaks and a new hydrogen bond to an oxygen atom of a nearby water molecule is formed, the $\text{O}-\text{H}$ stretch vibration will rapidly relax, which means that this reoriented vibration will no longer contribute to the anisotropy of the measured signal. Therefore, the anisotropy dynamics at delays > 3 ps represent the reorientation of the intact solvation structure only.

Since the observed reorientation results from the orientational diffusion of the intact shell, the dynamics can be described with the Stokes–Einstein relation for orientational diffusion. This description leads to the following expression for τ_{or} ,⁵⁶

$$\tau_{or}(T) = \frac{4\pi\eta(T)r_{h,solv}^3}{3kT} \quad (10)$$

with k being Boltzmann's constant, T being the temperature in Kelvin, $\eta(T)$ being the temperature-dependent viscosity, and $r_{h,solv}$ being the hydrodynamic radius of the solvation structure.

In Figure 4, the values of τ_{or} of the first hydration shell of the halogenic anions Cl^- , Br^- , and I^- are presented as a function of temperature. The solid curves in this figure are fits of eq 10 to the data. The temperature-dependent viscosities were obtained from the literature,⁷¹ leaving the radius $r_{h,solv}$ as the only fit parameter. This procedure results in $r_{h,solv}(\text{Cl}^-) = 213$ pm, $r_{h,solv}(\text{Br}^-) = 237$ pm, and $r_{h,solv}(\text{I}^-) = 205$ pm. These radii can be compared to the hydrodynamic radii obtained from the Stokes–Einstein relation for translational diffusion. From the ionic mobilities,⁷² it follows that $r_h(\text{Cl}^-) = 120$ pm, $r_h(\text{Br}^-) = 118$ pm, and $r_h(\text{I}^-) = 120$ pm. For all halogenic ions, r_h is significantly smaller than $r_{h,solv}$, which suggests that the ions show (translational) diffusion steps without their hydration shells, thus reducing the effective size of the diffusing ion. If $r_{h,solv}$ would equal r_h , the reorientation would be ~ 8 times as fast, with τ_{or} thus being only ~ 1 ps.

The value of $r_{h,solv}$ is smaller for I^- than for Br^- and Cl^- , which suggests that the size of the orientationally diffusing structure, i.e., the ion with its hydration shell, is smaller for I^- than for Cl^- and Br^- . It is not likely that the slower reorientation of the hydration shells of Cl^- and Br^- results from the formation of ion pairs, since it was found in dielectric relaxation studies that these pairs are formed only by a very small fraction of the ions present in solution.⁷³

The values of $r_{h,solv}$ are smaller than the anion–water hydrogen-bond length: $r_{HB}(\text{Cl}^-) = 323$ pm, $r_{HB}(\text{Br}^-) = 340$ pm, and $r_{HB}(\text{I}^-) = 360$ pm.⁶⁴ This deviation illustrates that the Stokes–Einstein relation, in particular, the viscosity entering this equation, is only truly applicable to macroscopic objects. In the case of diffusion solvation structures, the moving objects are of about equal size as the molecules of the viscous liquid. If the intermolecular interactions would have led to the same friction on the microscopic scale as on the macroscopic scale, the reorientation of the hydration shells would have been 5–10 times slower than observed. In spite of this large difference in magnitude between viscous interactions and molecular scale friction, the data can be fitted well to eq 10, which means that the molecular-scale friction and the macroscopic viscosity show a similar dependence on temperature.

2.5. Molecular Dynamics Simulations

Molecular dynamics simulations constitute a powerful and widely used method to get insight into the structure and dynamical behavior of aqueous solvation shells. An important parameter that is often derived from these studies is the residence time of the water molecules in the solvation shell of the ion. As can be expected, this residence time strongly depends on the nature of the solvated ion. For small positively charged ions like Li^+ , residence times up to several hundred picoseconds have been reported,¹⁹ whereas for large monovalent ions, much shorter residence times of ~ 10 ps have been found.^{8,9,12,14,16,20–24}

In the past, many different types of molecular dynamics simulations have been applied. Among these are classical molecular dynamics simulations using electrostatic pairwise potentials,^{8,19} simulations including polarizable water molecules and ions,^{9–12,14–16,20} mixed quantum-mechanical/molecular mechanical calculations,^{13,17,18} and full ab initio Car–Parrinello molecular dynamics simulations.^{21–24} In the latter type of calculations, all polarization and collective effects are included.

The structure and dynamics of the solvation shells of the Cl^- , Br^- , and I^- ions have been calculated with many different techniques. For the Cl^- ion, the calculated number of water molecules contained in the first solvation shell ranges between 5 and 6, depending on the precise definition of this shell. If the coordination number is obtained by integrating the first peak in the $\text{Cl}-\text{H}$ radial distribution function, the value is, in general, lower than when this number is obtained from the $\text{Cl}-\text{O}$ radial distribution function.²³ From the $\text{Cl}-\text{O}$ radial distribution function calculated with Car–Parrinello molecular dynamics simulation, a value of 5.6 was derived, in good agreement with the experimental value of 6.⁶² For Br^- , the average coordination number calculated with the Car–Parrinello approach was 6.3 (based on the $\text{Br}-\text{O}$ radial distribution function),²² in exact agreement with the experimental result.⁶² Calculations show the solvation shell of Br^- to be very dynamic; the coordination number was found to fluctuate between 4 and 8.²² For

I^- , the coordination number calculated with Car–Parrinello molecular dynamics simulations is 6.6 (based on the I–O radial distribution function).²⁴ This number is lower than is calculated in most other molecular dynamics simulation studies of aqueous I^- . The solvation structure of the I^- ion is calculated to be quite isolated from the local water structure. The average number of hydrogen bonds per water molecule in the shell is only 2.5. Of these hydrogen bonds, only 37% are formed with water molecules outside the shell. For comparison, the water molecules in the solvation shell of F^- form, on average, 3.1 hydrogen bonds, of which ~50% are formed with water molecules outside the shell. Hence, it can be concluded that the solvation shell of F^- integrates much better in the local water structure than the solvation shell of I^- . The different hydrogen bonding in the solvation shell of I^- is also apparent from the calculated blue-shift of the O–H stretch frequency of 70 cm^{-1} . This value is in excellent agreement with the experimental values obtained with double difference infrared spectroscopy⁶² and transient vibrational absorption spectroscopy (see Table 1).

The structure of the solvation shell strongly depends on the polarizabilities of the water molecules and the dissolved halogenic anion. Inclusion of these polarizabilities in the calculation makes the solvation structure strongly asymmetric²² and quite similar to that of a small gas-phase cluster of the halogenic anion and water, for which the ion is located at the surface of the cluster.^{10,11,15,21} The strong effect of polarizability on the calculated structure can be understood from the fact that the solvation structure is the result of the delicate competition between solvation interactions between ion and water molecules on one hand and hydrogen-bond interactions among the water molecules on the other hand.

The inclusion of polarizabilities of the water molecules and the ions in the calculation leads to a net (induced) dipole moment of the solvated ion. For Cl^- , Br^- , and I^- , the calculated dipole moment is ~1 debye.^{21–24} Interestingly, the inclusion of the polarizabilities of the water molecules and the anions has little effect on the dipole moments of the water molecules in the first solvation shell.^{22–24}

The definition of the residence time of water in the first hydration shell is delicate, as water molecules can leave the solvation shell for a short time only and return before a certain time has passed. A widely used definition is that these water molecules are still considered as being resident in the first solvation shell when the time spent outside the shell is <2 ps.⁸ The calculated residence time strongly increases upon the inclusion of polarization effects in the calculation. This is illustrated in Figure 5. In this figure, the residence correlation function for water in the solvation shell of Br^- is shown for the case where the residence correlation function is calculated with the Car–Parrinello approach (polarization effects included, dashed line) and for the case where the residence correlation function is calculated using a rigid SPC potential function for water (polarization effects not included, dotted–dashed line). If polarization effects are included, the residence time constant is ~19 ps; if not, the residence time constant is only 5 ps. For Cl^- , similar effects are observed. If polarization effects are not included, the residence time in the first solvation shell calculated with classical molecular dynamics (MD) simulations is quite short, only 4.5 ps.⁸ Inclusion of the polarization effects on the ion and the water molecules in a classical MD simulation makes the residence time 2–3 times longer.^{9,12,14,16,20} In Figure 6, the residence correlation function calculated with the Car–Parrinello

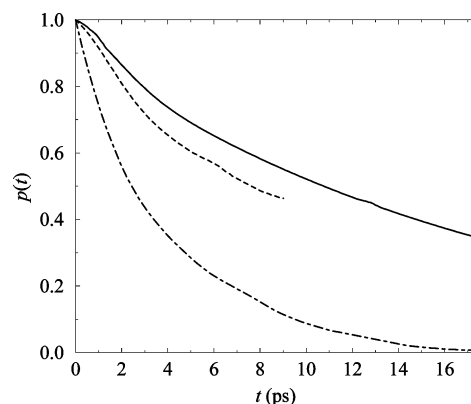


Figure 5. Calculated residence time correlation function for the aqueous solvation shell of Br^- . Solid line, HBr, calculated with the Car–Parrinello method; dotted line, Br^- , calculated with the Car–Parrinello method; dashed–dotted line, Br^- , calculated with classical molecular dynamics simulations using a nonpolarizable force field. Reprinted with permission from ref 22. Copyright 2002 American Institute of Physics.

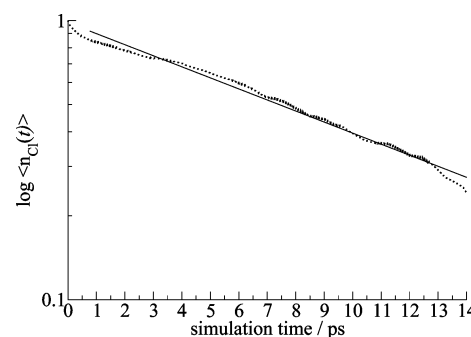


Figure 6. Logarithmic plot of the time-averaged residence time correlation function (dotted line) and the monoexponential fit (solid line) to this function with a characteristic time constant of 12 ps. Reprinted with permission from ref 23. Copyright 2003 American Institute of Physics.

approach for Cl^- is presented.²³ An exponential fit to this function gives a residence time constant of 12 ps. For I^- , a residence time of ~7.5 ps is calculated both in classical and in Car–Parrinello molecular dynamics simulations.^{16,24}

Recently, the orientational dynamics of water molecules in the first hydration shell of Cl^- have been studied with classical molecular dynamics simulations.⁷⁰ In this study, the reorientation of the O–H groups interacting with Cl^- was calculated to be dominated by a fast rotation out of the solvation shell with a time constant of 3.3 ps. The intact hydrogen-bonded O–H... Cl^- system was found to show a relatively slow reorientation with a time constant of 6.2 ps for a solution containing 1 M NaCl. The two processes together lead to an effective reorientation time constant of 2.2 ps for the O–H groups solvating the Cl^- ion, which is faster than the molecular reorientation in bulk liquid water. The mechanism of the out-of-shell rotation was found to be a jump mechanism in which the hydrogen bond to the Cl^- ion is broken and a new hydrogen bond to another water molecule is formed. The transition state of this reorientation is a bifurcated hydrogen bond between the O–H group of the rotating water molecule, the Cl^- ion, and the other water molecule.

2.6. Discussion

In Table 2, the residence time constants obtained with NMR and molecular dynamics simulations are presented

Table 2. Residence Times and/or Characteristic Time Scales of the Hydrogen-Bond Fluctuations of the Hydration Shells of Cl^- , Br^- , and I^- Obtained with Different Methods

	Cl^- (ps)	Br^- (ps)	I^- (ps)
Car–Parrinello MD	12	19	7.5
NMR	15	10	5
transient IR	12 ± 3	25 ± 5	18 ± 5

together with the correlation time constants of the hydrogen-bond length fluctuations measured with transient vibrational spectroscopy. For the hydration shells of Cl^- and Br^- , the residence time and the time constant of the hydrogen-bond fluctuations are quite similar. This good comparison suggests that the dissociation of a water molecule from the hydration shell results from the fluctuations in the length of the hydrogen bond. However, the residence time and the time scale of the hydrogen-bond fluctuations are in fact very different parameters, as will be discussed in the following.

An effect that could make the residence time significantly shorter than the time constant of the hydrogen-bond fluctuations is the out-of-shell rotation of the water molecule followed by the formation of a new hydrogen bond to an oxygen atom of a neighboring water molecule. Here it should be reminded that the hydrogen-bond fluctuation time constants as specified in Table 2 are a property of the intact $\text{O}-\text{H}\cdots\text{X}^-$ system. The formation of an $\text{O}-\text{H}\cdots\text{O}$ hydrogen bond will lead to rapid vibrational relaxation ($T_1 = 0.8$ ps) of the $\text{O}-\text{H}$ stretch vibration, as a result of which the oscillator will disappear from the signal.⁷⁰ Therefore, out-of-shell rotation leading to the direct formation of an $\text{O}-\text{H}\cdots\text{O}$ is not contained in the time constant of the observed hydrogen-bond length fluctuations, but it will contribute to a shortening of the residence time.

In a recent molecular dynamics study, the water molecules in the hydration shell of Cl^- were found to show both a rapid out-of-shell rotation with a time constant of 3.3 ps and a slower reorientation due to the frame rotation of the intact $\text{O}-\text{H}\cdots\text{Cl}^-$ system.⁷⁰ The calculated time constant of this latter rotation is 10 ps for a 3 M solution, which is in excellent agreement with the time constant of 9.6 ps found for this process with polarization-resolved transient vibrational spectroscopy. The fast out-of-shell rotation with a time constant of ~ 3 ps appears to be inconsistent with the results of other studies. As discussed above, rotation out of the shell implies that the water molecule leaves the hydration shell. Therefore, an out-of-shell rotation with 3.3 ps is not consistent with the results of other (Car–Parrinello) molecular dynamics simulations that find the residence time of water molecules in the hydration shell of Cl^- to be ~ 10 ps.

Out-of-shell rotation with a time constant of ~ 3 ps also appears to be at odds with the results from isotropic transient vibrational spectroscopy studies. An out-of-shell rotation affects the dynamics of the isotropic signal measured in transient vibrational spectroscopy, because this rotation turns the slowly relaxing $\text{O}-\text{H}\cdots\text{Cl}^-$ system into a rapidly relaxing $\text{O}-\text{H}\cdots\text{O}$ system. Hence, the observed vibrational relaxation rate will be the sum of two channels, one being the intrinsic relaxation of the intact $\text{O}-\text{H}\cdots\text{X}^-$ system and the other formed by out-of-shell rotation followed by fast relaxation. The intrinsic lifetime of the intact $\text{O}-\text{H}\cdots\text{X}^-$ is expected to increase going from Cl^- to Br^- to I^- , while the out-of-shell rotation is expected to decrease in this series. In the experiment, the vibrational lifetime is observed to increase in the halogenic series (see next section). Hence, the

vibrational relaxation appears to be dominated by the intrinsic relaxation of the intact $\text{O}-\text{H}\cdots\text{X}^-$ system, which implies that the out-of-shell rotation should be much slower than the observed vibrational lifetimes of 2.3–4.5 ps (see next section).⁶¹

An estimate of the out-of-shell rotation time can be obtained from a comparison of the vibrational lifetimes measured at low and high salt concentrations. With increasing salt concentration, the out-of-shell rotation will decelerate, as it requires the approach of the $\text{O}-\text{H}\cdots\text{X}^-$ system by another water molecule to form a bifurcated hydrogen-bonded transition state.⁷⁰ At high salt concentrations, this formation is expected to become increasingly sterically hindered, leading to a slowing down of the out-of-shell rotation. If we assume that the change in vibrational relaxation time constant of $\text{O}-\text{H}\cdots\text{Cl}^-$ from 2.2 ps at low concentrations to 2.6 ps at high concentrations is entirely due to the slowing down of the out-of-shell rotation, we find a time constant $\tau_{\text{OOS}}(\text{Cl}^-)$ for this rotation at low salt concentrations of $1/[(1/2.2) - (1/2.6)] = 11$ ps. Similarly, we find $\tau_{\text{OOS}}(\text{Br}^-) = 1/[(1/2.5) - (1/3.6)] = 8$ ps and $\tau_{\text{OOS}}(\text{I}^-) = 1/[(1/2.5) - (1/3.6)] = 6$ ps. These time constants suggest that the dissociation of water from the shell may be dominated by out-of-shell rotation, which would imply that there is no direct connection between the residence time and the time constant τ_c of the fluctuations of the intact $\text{O}-\text{H}\cdots\text{X}^-$ bond. The fact that these time constants are nevertheless comparable, at least for the hydration shells of Cl^- and Br^- (Table 2), suggests that the out-of-shell rotation and the $\text{O}-\text{H}\cdots\text{X}^-$ hydrogen-bond length fluctuations find a common origin in the relative motions of the water molecules in the first and the second hydration shells.

For the hydration shell of I^- , the different techniques arrive at somewhat different values for the residence time/time constant of the hydrogen-bond fluctuations. For this shell, NMR and molecular dynamics simulations arrive at a much shorter time constant (5–7 ps) than transient vibrational spectroscopy (18 ± 5 ps). This difference can be assigned to the rotation of the water molecules out of the hydration shell of I^- being faster than the length modulations of the intact $\text{O}-\text{H}\cdots\text{I}^-$ hydrogen bond.

3. Energy Dynamics of Ionic Hydration Shells

3.1. Introduction

For bulk water, the vibrational energy relaxation time constant T_1 of the $\text{O}-\text{H}$ stretch vibrations of the water molecules has been observed to be strongly dependent on the strength and nature of the hydrogen bonds.^{34,74} Therefore, it can be expected that the structures of ionic hydration shells will also affect the rate of vibrational-energy relaxation. A technique ideally suited to measure the vibrational energy relaxation of the molecular vibrations is transient vibrational absorption spectroscopy. In this section, we give an overview of the information on the energy dynamics of ionic hydration shells obtained with this technique.

3.2. Vibrational Relaxation of Anionic Hydration Shells

The vibrational energy relaxation of water molecules has been studied for several alkali halide solutions.^{53–55,57,58,61} These solutions consist of a low concentration of 0.1 M HDO in D_2O and different concentrations (0.5, 1, 2, 3, 6, 9, and 10 M) of KF, NaCl, NaBr, and NaI.

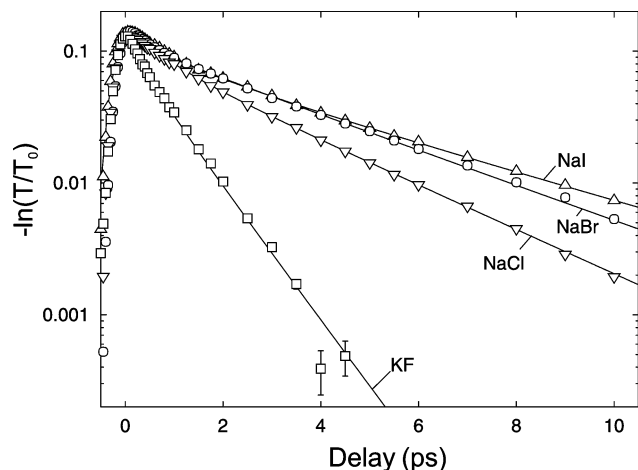


Figure 7. Pump-probe transients measured for aqueous solutions of different salts in HDO/D₂O. The transients were measured using a pump frequency of 3450 cm⁻¹ resonant with the $\nu = 0 \rightarrow 1$ transition and a probe frequency of 3200 cm⁻¹, resonant with the $\nu = 1 \rightarrow 2$ transition. Reprinted with permission from ref 58. Copyright 2002 Elsevier.

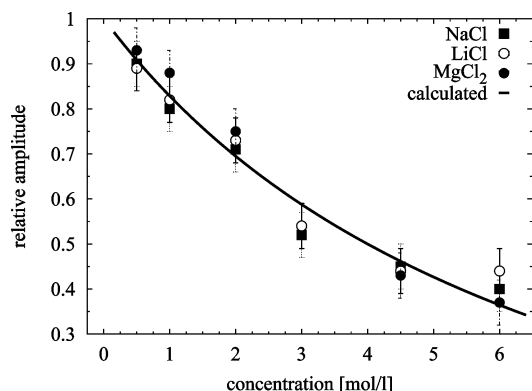


Figure 8. Relative abundance of the fast component for a series of Cl⁻ salts as a function of concentration, measured at a probe frequency of 3450 cm⁻¹. The line is obtained from a simple calculation of the relative abundance of the fast component, assuming a coordination number of 6 of the Cl⁻ ion and a cross-sectional ratio of the Cl⁻ and water-bound HDO molecules of 2.2 at a frequency of 3450 cm⁻¹.

In Figure 7, pump-probe transients measured for four different salt solutions are shown. For the solutions of NaCl, NaBr, and NaI, the data can be fitted well with a biexponential function. Two time constants are obtained, of which the shorter has a value of ~ 0.8 ps and is the same for all salt solutions. This value compares very well with the vibrational relaxation time constant of the O-H stretch vibration of pure HDO/D₂O.^{34,75} This component originates from O-H groups that form O-H \cdots O hydrogen bonds to other water molecules. As a result, the relaxation behavior is very similar to that of the O-H groups in HDO/D₂O. The fast component also contains the response of the HDO molecules in the first hydration shell of the Na⁺ cations, because for the HDO molecules near the cation, the O-H groups will point away from the ion and will form O-H \cdots O hydrogen bonds with bulk D₂O molecules.⁷⁶⁻⁷⁸

In Figure 8, the relative abundance of the fast component is plotted as a function of the salt concentration for solutions of NaCl, LiCl, and MgCl₂. It is seen that, with increasing salt concentration, the amplitude of the fast component decreases while the amplitude of the slow relaxation component increases. The time constant of the slow com-

ponent depends on the type of anion. For solutions of 6 M NaCl, NaBr, and NaI, we find time constants of 2.6 ± 0.3 ps, 3.4 ± 0.3 ps, and 3.9 ± 0.3 ps, respectively, thus showing an increase within the halogenic series from Cl⁻ to Br⁻ to I⁻. In view of these observations, the second relaxation component is assigned to HDO molecules that solvate the halogenic anion via the formation of an O-H \cdots X⁻ hydrogen bond (with X⁻ = Cl⁻, Br⁻, I⁻). This means that the time constant of the second component corresponds to the vibrational lifetime T_1 of O-H, the vibration of HDO molecules that are hydrogen bonded with their O-H group to the anion. For KF, the relaxation is observed to be single exponential with a time constant of 0.8 ± 0.2 ps. This observation shows that HDO molecules that are hydrogen bonded to F⁻ show approximately the same rate of vibrational relaxation as HDO molecules that are hydrogen bonded to D₂O.

The dependence of the vibrational lifetime of the slow component on the nature of the anion suggests that the O-H \cdots X⁻ hydrogen bond (X⁻ = Cl⁻, Br⁻, I⁻) is involved in the vibrational relaxation mechanism. In Figure 1, it was shown that the frequency of the O-H vibration of the O-H \cdots X⁻ hydrogen-bonded system increases in the halogenic series Cl⁻, Br⁻, and I⁻. This increase in frequency indicates that the hydrogen bond becomes weaker.⁶³⁻⁶⁵ A weaker hydrogen-bond interaction in turn leads to a decrease of the anharmonic interaction between the O-H stretch vibration and the hydrogen-bond mode,⁷⁹ which causes the slowing down of the vibrational relaxation. In addition, the reduced mass of the O-H \cdots X⁻ hydrogen-bond stretch vibration, which determines the energy spacing of the levels of this mode, increases within the halogenic series Cl⁻, Br⁻, I⁻. The hydrogen-bond frequencies have been measured to be 210 cm⁻¹ for O-H \cdots Cl⁻, 158 cm⁻¹ for O-H \cdots Br⁻, and 135 cm⁻¹ for O-H \cdots I⁻.⁸⁰ Therefore, the dissipation of the excitation energy of the O-H stretch vibration will involve a higher level of excitation of the hydrogen-bond vibration for I⁻ than for Cl⁻, which leads to a decrease of the (resonant) part of the anharmonic coupling that is responsible for the relaxation.⁸¹ For a solution of KF in HDO/D₂O, the absorption spectrum is slightly red-shifted with respect to the spectrum of HDO/D₂O, which indicates that the O-H \cdots F⁻ hydrogen bond is even stronger than the O-H \cdots O hydrogen bond. The resulting strong anharmonic interaction between the O-H vibration and the O-H \cdots F⁻ hydrogen bond makes the vibrational lifetime of HDO solvating F⁻ relatively short, thus explaining the absence of a slow relaxation component for a solution of KF in HDO/D₂O.

3.3. Effect of Concentration on the Energy Dynamics of the Anionic Hydration Shell

In Figure 9, pump-probe traces of solutions containing different concentrations of NaI are shown. It is observed that the time constant T_1 of the vibrational relaxation of the O-H group of the O-H \cdots I⁻ systems shows a significant dependence on concentration: T_1 increases from 2.4 ± 0.2 ps at 0.5 M to 4.7 ps at 10 M.

In Figure 10, T_1 is plotted as a function of anion concentration for a series of lithium salts. For all anions, the lifetime rises with concentration, but the slope of the rise increases going from Cl⁻ to Br⁻ to I⁻. Below 3 M, the lifetimes of Br⁻ and I⁻ are almost the same; Cl⁻ is faster at all measured concentrations. Sodium and magnesium salts also show an increase of T_1 with increasing concentration of dissolved salt.

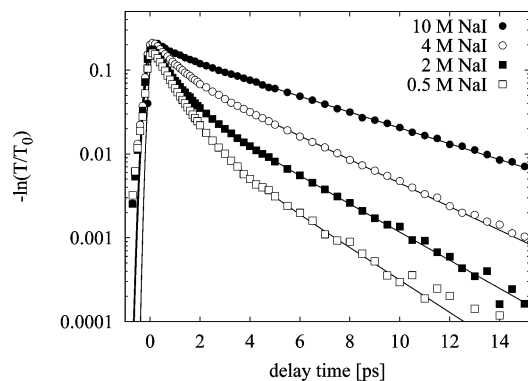


Figure 9. Pump-probe traces of solutions of several concentrations of NaI in HDO/D₂O. The measurement was performed at a pump frequency of 3450 cm⁻¹ and a probe frequency of 3200 cm⁻¹. The lines are fits to the data. The fit function is a biexponential function convolved with a Gaussian cross-correlation function.

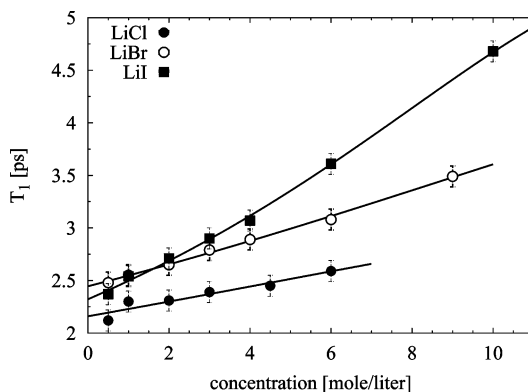


Figure 10. T_1 of the O-H stretch vibration of the O-H \cdots X⁻ system (X⁻ = Cl⁻, Br⁻, or I⁻) as a function of concentration for three salts containing the same cation: LiCl, LiBr, and LiI. The lines are guides to the eye.

The dependence of T_1 of the O-H \cdots X⁻ system on concentration has been explained from the coupling between the different types of hydrogen bond modes in the liquid.⁶¹ The hydrogen bonds are similar in frequency and will be coupled, leading to the formation of delocalized modes. This notion also applies to the hydrogen bond that involves the hydrogen atom of the relaxing O-H group in the O-H \cdots X⁻ system, and that likely plays an important role in the vibrational relaxation of the O-H stretch vibration. This hydrogen bond will not be a pure local O-H \cdots X⁻ hydrogen bond but will show admixtures of neighboring O-D \cdots O and O-H \cdots O hydrogen bond modes. These admixtures will affect the rate of vibrational relaxation of the O-H stretch vibration.

An alternative explanation of the observed increase of T_1 with concentration is formed by a slowing down of the out-of-shell rotation. The rotation of the O-H group out of the hydration shell will contribute to the vibrational relaxation of the O-H \cdots X⁻ system. This rotation results in the breaking of the O-H \cdots X⁻ hydrogen bond and the formation of a new O-H \cdots O hydrogen bond to a neighboring water molecule. The latter system will show a relatively rapid vibrational relaxation with a time constant of 0.8 ps. As the out-of-shell rotation is expected to be slower than this relaxation, the overall rate of this additional relaxation channel is determined by the rate of the out-of-shell rotation. The out-of-shell rotation is expected to be concentration dependent, as it requires the approach of the O-H \cdots X⁻ system by another

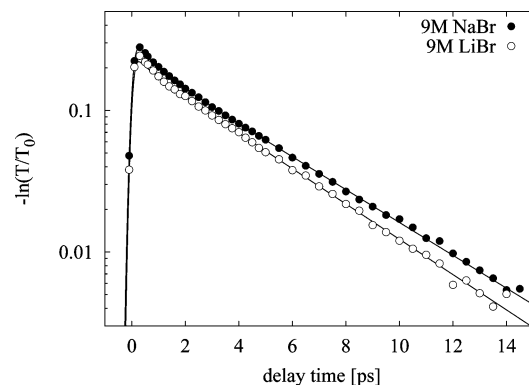


Figure 11. Pump-probe traces of 9 M solutions of LiBr and NaBr in HDO/D₂O. The measurement was performed at a pump frequency of 3450 cm⁻¹ and a probe frequency of 3200 cm⁻¹. The lines are fits to the data. The fit function is a biexponential function convolved with a Gaussian cross-correlation function.

water molecule to form a bifurcated hydrogen-bonded transition state.⁷⁰ With increasing concentration, this approach will be slowed down, and at high concentration, it may even become impossible. In the previous section, it was shown that, if the difference in T_1 at low and high concentrations would be completely due to the vanishing of the out-of-shell rotation, $\tau_{\text{os}}(\text{Cl}^-) = 1/[(1/2.2) - (1/2.6)] = 11$ ps, $\tau_{\text{os}}(\text{Br}^-) = 1/[(1/2.5) - (1/3.6)] = 8$ ps, and $\tau_{\text{os}}(\text{I}^-) = 1/[(1/2.5) - (1/3.6)] = 6$ ps. These time constants decrease going from Cl⁻ to Br⁻ to I⁻, which is consistent with the fact that the hydration shell becomes more labile in the halogenic series.

3.4. Effect of Cations on the Energy Dynamics of the Anionic Solvation Shell

It can be expected that the vibrational lifetime of water molecules in the solvation shell of the anion depends on not only the nature of the anion and the concentration but also the nature of the cation, in particular when the hydration shell is shared by the anion and the cation, thus forming Y⁺O-H \cdots X⁻ systems.

In Figure 11, it is shown that the vibrational relaxation is somewhat faster for a Br⁻ solution with Li⁺ as the counterion than with Na⁺ as the counterion. Interestingly, in a study of the vibrational relaxation of NaCl and LiCl solutions,⁵⁵ the solution containing Li⁺ ions was found to show a *slower* vibrational relaxation. However, in a comment on this paper, it was shown that this result is not statistically significant.⁵⁷ In the same comment, it was shown that, for Cl⁻ solutions also, the relaxation is, in fact, slightly faster with Li⁺ than with Na⁺ as the counterion, in agreement with the results found for the Br⁻ solutions shown in Figure 11. For solutions containing Mg²⁺, the relaxation is observed to be even faster than for solutions containing Li⁺.⁶¹ Hence, the vibrational lifetime of HDO solvating Cl⁻ and Br⁻ is observed to decrease in the cationic series Na⁺, Li⁺, Mg²⁺.

The effect of cations on the vibrational lifetime of the anionic hydration shell can be explained from the electric fields exerted by the cations. The electric field of the cation polarizes the O-H \cdots O and O-H \cdots X⁻ hydrogen bonds of water molecules adjacent to the cation. With increasing polarization, the strength of the hydrogen bonds increases, which in turn leads to an increase of the anharmonic interaction with the O-H stretch vibration of an HDO molecule solvating the X⁻ anion. The Li⁺ ion is smaller than Na⁺, while Mg²⁺ has a similar size as Na⁺ but possesses

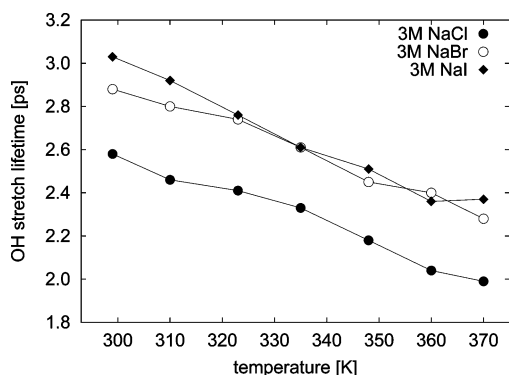


Figure 12. O–H stretch lifetime of anion-bound water molecules as a function of temperature for 3 M solutions of Cl^- , Br^- , and I^- in liquid water. Reprinted with permission from ref 58. Copyright 2002 Elsevier.

twice the charge. Therefore, the local electric field exerted by the cation increases going from Na^+ to Li^+ to Mg^{2+} , thereby explaining the observed decrease of the vibrational lifetime of the anionic hydration shell in this series.

3.5. Temperature Dependence of the Energy Dynamics of the Anionic Solvation Shell

In Figure 12, the anion-bound O–H stretch lifetimes of Cl^- , Br^- , and I^- are shown as a function of temperature. For all anions, the vibrational lifetime decreases with temperature. Such a decrease of the vibrational lifetime with temperature is quite generally observed and can be explained from the increase of the anharmonic interaction with increasing thermal occupation of the accepting modes.⁸¹

Interestingly, previous work on the O–H stretch vibration of bulk liquid water (i.e., $\text{HDO}/\text{D}_2\text{O}$ ³⁴ and H_2O ⁷⁴) showed that the lifetime of the O–H stretch vibration of bulk water *increases* with temperature. In recent theoretical work on the vibrational relaxation of $\text{HDO}/\text{D}_2\text{O}$, it was found that this increase of T_1 with temperature can be largely explained from the increase of the energy gap to the overtone of the bending mode.⁸⁷

The opposite temperature dependence of the vibrational relaxation of $\text{O}-\text{H}\cdots\text{O}$ and $\text{O}-\text{H}\cdots\text{X}^-$ ($\text{X}^- = \text{Cl}^-$, Br^- , and I^-) can be explained from the temperature dependence of the O–H stretch absorption spectra of the $\text{O}-\text{H}\cdots\text{O}$ oscillators and the $\text{O}-\text{H}\cdots\text{I}^-$ oscillators. The latter spectrum is constructed in the following way. First a difference spectrum is taken of the spectrum of a solution of 6 M NaI, 1 M HDO, and the D_2O spectrum of a solution of 6 M NaI in D_2O . This difference spectrum contains the response of all different types of O–H oscillators, i.e., O–H hydrogen bonded to D_2O and O–H hydrogen bonded to I^- . Then, a second difference spectrum is obtained by taking the difference of the spectrum of a solution HDO in D_2O and that of pure D_2O . This difference spectrum represents only O–H oscillators hydrogen bonded to D_2O . To obtain a spectrum that is representative for the $\text{O}-\text{H}\cdots\text{I}^-$ oscillators, the second difference spectrum is subtracted from the first. The spectra are shown in Figure 13. For the $\text{O}-\text{H}\cdots\text{O}$ oscillators of pure water, the O–H band shows a strong blue-shift of $\sim 50\text{ cm}^{-1}$ when the temperature is increased from room temperature to 93 °C. In contrast, the O–H stretch band of $\text{O}-\text{H}\cdots\text{I}^-$ oscillators shifts by only 10 cm^{-1} in this temperature range. This means that the hydrogen bonds of the solvation shell become only slightly weaker when the temperature is increased toward the boiling point. As a result, the temper-

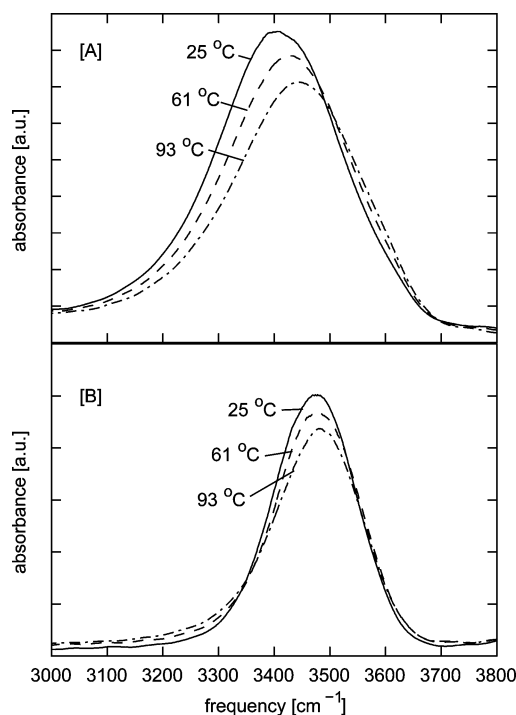


Figure 13. Spectra of the O–H stretch vibration of $\text{HDO}/\text{D}_2\text{O}$ (the D_2O background was subtracted, panel A) and of a solution of 6 M NaI in $\text{HDO}/\text{D}_2\text{O}$ (background D_2O and bulk O–H band were subtracted, panel B) at three temperatures. For $\text{HDO}/\text{D}_2\text{O}$, the band shifts to the blue by $\sim 50\text{ cm}^{-1}$, the $\text{O}-\text{H}\cdots\text{X}^-$ band shifts only by $\sim 10\text{ cm}^{-1}$. Reprinted with permission from ref 58. Copyright 2002 Elsevier.

ature effect on the vibrational lifetime $\text{O}-\text{H}\cdots\text{X}^-$ oscillators ($\text{X}^- = \text{Cl}^-$, Br^- , I^-) is dominated not by an increase of the energy gap ($\sim 500\text{ cm}^{-1}$) with the overtone of the bending mode but rather by the increased thermal occupation of other, low-frequency accepting modes (i.e., hydrogen bonds).⁸¹ As a result, T_1 decreases with temperature for the $\text{O}-\text{H}\cdots\text{X}^-$ hydrogen-bonded systems.

4. Structural Dynamics of Water Outside the First Ionic Hydration Shell

4.1. Introduction

Ions are believed to have a long-range effect on the structure of liquid water, either strengthening the hydrogen-bond network of water (structure making) or weakening this network (structure breaking).⁵ A strong indication for a structure making and breaking effect of ions on liquid water is the influence of ions on the viscosity of water.⁶ The Jones–Dole expression⁸⁸ for the viscosity of aqueous ionic solutions states that, for concentrations up to $\sim 1\text{ M}$,

$$\frac{\eta - \eta_0}{\eta_0} \approx A\sqrt{c} + Bc \quad (11)$$

with η being the viscosity of the solution, η_0 being the viscosity of pure water, c being the ion concentration, and A and B being constants. The first term on the right-hand side results from electrostatic interactions between the ions. The magnitude of A can be easily calculated,⁸⁹ as it is assigned to the electrostatic interaction between the ions. The second term is attributed to the influence on the hydrogen bond structure by the ion: some ions, like the tetraalkylam-

monium ions and ions with high charge densities, have large positive B coefficients and are, thus, believed to be strong structure makers, while other ions, in particular ions with low charge densities, have negative B coefficients and are believed to be structure breaking.

Another indication for a structure making and breaking effect of ions on liquid water is formed by the anomalous mobility of many ions in water. The Zwanzig model for ionic mobilities, which accounts for the hydrodynamic size of an ion and the polarizability of the solvent,⁹⁰ gives a poor quantitative description of most ionic mobilities in water. In general, ions with low charge densities (e.g., large univalent ions) have a larger mobility than predicted by the Zwanzig equation.⁷ Ions with high charge densities generally have a smaller mobility than predicted by the Zwanzig equation. These observations also suggest that ions with high charge densities enhance the hydrogen-bond network of liquid water.

The above-described observations that are in support of a structure making or breaking effect of ions on water are based on macroscopic properties of the liquid (viscosity and conductivity). Hence, these properties represent averages over the whole liquid, making it impossible to discern the specific properties of the hydration shells from those of the hydrogen-bond network of the liquid outside these shells. Fortunately, there exist spectroscopic techniques that do allow for such a distinction and that provide molecular-scale information on the effects of ions on the hydrogen-bond network of liquid water. In this section, we will present and discuss the results obtained with several spectroscopic techniques and molecular dynamics simulations on the long-range effect of ions on the structural dynamics of liquid water, i.e., the properties of the liquid *outside* the first hydration shells of the ions.

4.2. Low-Frequency Raman Scattering and Optical Kerr Effect

The low-frequency Raman spectrum of aqueous salt solution represents the dynamics of the structural relaxation processes of the whole liquid.^{91–94} Hence, this spectrum gives information on the strength and stability of the hydrogen-bond network. The measured low-frequency dielectric response is often fitted to a Cole–Cole type relaxation,

$$\chi(\nu) = \frac{\epsilon_{CC}(c) - \epsilon_{\infty}}{1 + (i2\pi\nu\tau_{CC})^{\beta}} \quad (12)$$

with τ_{CC} being the (structural) relaxation time and β being a parameter that accounts for the presence of a distribution of relaxation times. In the case where $\beta = 1$, there is only a single relaxation time τ and the Cole–Cole relaxation is the same as a Debye relaxational mode.

For most salt solutions, β is found to be ~ 0.9 , which implies that there is not a broad distribution of relaxation times. The measured time constants are ~ 1 ps, which is substantially shorter than the time constants of the translational and orientational dynamics of the hydration shells. For all solutions, it is found that the time constant τ increases with increasing salt concentration.^{91–94} It is also found that the time constant correlates well with the viscosity of the liquid. The largest relaxation time constants are found for solutions containing ions like Mg^{2+} .

The time-resolved measurement of the optical Kerr effect⁹⁵ provides similar information on the relaxation

dynamics of aqueous salt solutions as the measurement of the low-frequency Raman spectrum. In experiments on solutions of HCl in water, two relaxation time constants were observed. The shortest one is ~ 1 ps and is very similar to the time constant deduced from the measurement of the low-frequency Raman spectrum. The second one ranges from 2 to 7 ps, depending on temperature and concentration. Both time constants scale well with the viscosity, although the correlation is not perfect for the shortest time constant at low temperatures. The short time constant is assigned to local liquid dynamics, i.e., like the breaking and formation of a local hydrogen bond. The longer time scale is assigned to the collective relaxation of highly connected hydrogen-bonded groups of molecules.

4.3. Dielectric Relaxation and Low-Frequency Infrared Spectroscopy

In dielectric relaxation spectroscopy, the polarization response to an applied electric field is measured as a function of frequency. This polarization response predominantly results from the reorientation of the dipolar water molecules. The frequency spectrum of the polarization response thus provides information on the strength and rigidity of the hydrogen-bond network of the liquid. The typical frequency range in which this technique is applied is from 0 to 100 GHz.

In dielectric relaxation spectroscopy, the relative dielectric permittivity $\epsilon'(c, \nu)$ and the total loss $\rho''(c, \nu)$ are measured as a function of the concentration c of dissolved salt and of frequency ν . $\rho''(c, \nu)$ is related to the dielectric loss $\epsilon''(c, \nu)$ by

$$\rho''(c, \nu) = \epsilon''(c, \nu) + \kappa/(2\pi\nu\epsilon_0) \quad (13)$$

with κ being the conductivity and ϵ_0 being the vacuum permittivity. The conductivity contribution dominates at low frequencies and determines the minimum frequency at which $\epsilon''(c, \nu)$ can be determined. The technique has been applied to many aqueous salt and acid solutions.^{73,85,86,96,97} In Figure 14, typical measurement results obtained for solutions of different concentrations NaBr in water are presented. It is shown that the dielectric response decreases with increasing concentration of dissolved salt.

The frequency-dependent $\epsilon'(c, \nu)$ and $\epsilon''(c, \nu)$ are used to determine the static dielectric constant $\epsilon(c, 0)$. The addition of salt to water will, in general, lead to a decrease of the static dielectric response. This decrease consists of two contributions:

$$\Delta\epsilon(c, 0) = \epsilon(0, 0) - \epsilon(c, 0) = \Delta\epsilon_{eq}(c, 0) + \Delta\epsilon_{kd}(c, 0) \quad (14)$$

The term $\Delta\epsilon_{eq}(c, 0)$ predominantly represents the loss in dielectric response due to the water molecules that are immobilized in the solvation shells of the ions. These water molecules will no longer contribute to the polarization response of the water to an applied electric field. An additional minor contribution to $\Delta\epsilon_{eq}(c, 0)$ results from a dilution effect: in a salt solution, part of the volume is taken by ions that have a lower dielectric response ($\epsilon_{ion}(0) \approx 2$) than water. The term $\Delta\epsilon_{kd}(c, 0)$ is the so-called kinetic depolarization term.⁹⁸ This term finds its origin in the rotation of the dipolar solvent molecules that is induced by the migration of the ions in the applied electric field. This rotation sets up a polarization in the direction opposite to

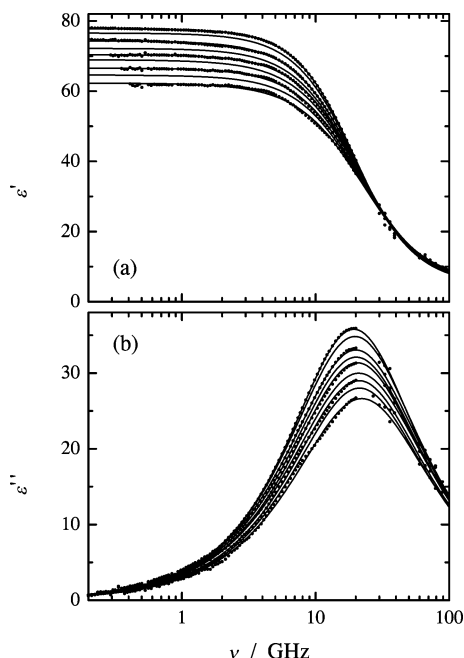


Figure 14. Dielectric permittivity (a) and loss (b) curves for a solution of NaBr in water at room temperature. The concentrations are 0.05, 0.15, 0.35, 0.50, 0.65, 0.80, 1.00, 1.20, 1.40 M (top to bottom). Reproduced with permission from ref 73. Copyright 2005 American Chemical Society.

the normal dipolar alignment in the applied field, thus leading to a decrease of the dielectric constant. This contribution is proportional to the conductivity and the Debye relaxation time of the solvent:

$$\Delta\epsilon_{\text{kd}}(c, 0) = p\kappa(c, 0) \frac{\epsilon(0, 0) - \epsilon_{\infty}(c, 0)}{\epsilon(0, 0)} \frac{\tau(0)}{\epsilon_0} \quad (15)$$

The factor p accounts for the hydrodynamic boundary conditions of stick ($p = 1$) or slip ($p = 2/3$) ionic motion. The time constant $\tau(0)$ is the Debye time constant of the pure solvent. Both $\Delta\epsilon_{\text{eq}}(c, 0)$ and $\Delta\epsilon_{\text{kd}}(c, 0)$ contribute to the loss in dielectric response.

Since $\Delta\epsilon_{\text{eq}}(c, 0)$ mainly represents the loss of dielectric response due to the binding of water to the ions, its value can be used to determine the number of water molecules that bind to the ions. The determination of $\Delta\epsilon_{\text{eq}}(c, 0)$ requires the determination of the magnitude of $\Delta\epsilon_{\text{kd}}(c, 0)$, since the measured change in dielectric response is the sum of both. $\Delta\epsilon_{\text{kd}}(c, 0)$ depends on the hydrodynamic boundary condition of stick or slip ionic motion. In the case of stick ionic motion, $\Delta\epsilon_{\text{kd}}(c, 0)$ would become quite high, meaning that $\Delta\epsilon_{\text{eq}}(c, 0)$ would become unreasonably small. This would have, as a consequence, that the ions acquire very low or even negative solvation numbers. Hence, the kinetic depolarization must occur under slip boundary conditions.⁸⁵

The frequency dependence of the dielectric susceptibility $\epsilon(\nu)$ measured at a particular concentration can be fitted to the expression for the Cole–Cole response of eq 12.^{73,85,86,96,97} In Figure 15, the time constant τ_{CC} is presented as a function of concentration for five different salt solutions. For all salts, the value of τ_{CC} is observed to decrease with increasing concentration.⁷³ This result has also been found in previous studies of NaCl solutions.^{85,97} The decrease of τ_{CC} with increasing concentration suggests that the hydrogen-bond network of the liquid becomes weaker, because a weaker

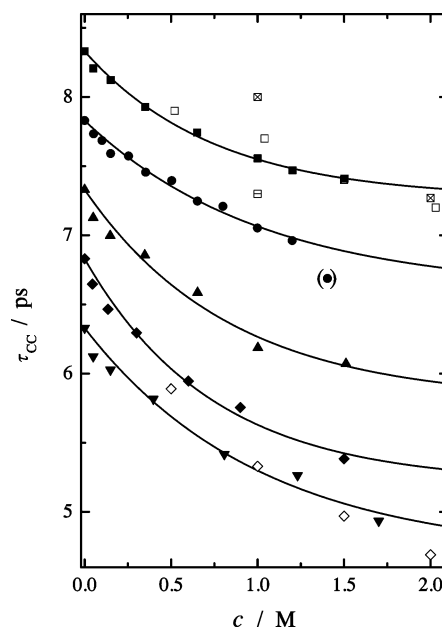


Figure 15. Concentration dependence of the relaxation times τ_{CC} for aqueous solutions of sodium salts at room temperature. The τ_{CC} have been shifted vertically by varying amounts for clarity: NaNO₃ (black squares), NaBr (black circles, -0.5 ps), NaI (black triangle, -1.0 ps), NaClO₄ (black diamond, -1.5 ps), NaSCN (black downward triangle, -2.0 ps). Also included are literature data for NaNO₃ (cross-hatch square,⁹⁹ open square,¹⁰⁰ and horizontal line square¹⁰¹) and NaClO₄ (open diamond¹⁰²). Reproduced with permission from ref 73. Copyright 2005 American Chemical Society.

hydrogen-bond network will give rise to faster orientational motion of the water molecules.

The dependence of τ_{CC} on concentration can be fitted well with the function⁷³

$$\tau_{\text{CC}}(c) = A e^{-kc} + (\tau_{\text{CC}}(0) - A) \quad (16)$$

where $\tau_{\text{CC}}(0)$ is the relaxation time constant for pure water, $\tau_{\text{CC}}(0) = 8.3$ ps.^{103,104} The value of k , which represents the sensitivity of the relaxation time constant to the concentration, scales quite well with the radius of the dissolved anion. This result suggests that the hydrogen-bond network of water gets more strongly broken with increasing size of the dissolved anions.

The frequency range of the dielectric relaxation measurements was extended to 1.3 THz (40 cm^{-1}) in a low-frequency infrared absorption study of aqueous solutions of LiCl.¹⁰⁵ In this study, it was also found that the water molecules contained in the solvation shells of the ions no longer contribute to the low-frequency dielectric response. As a result, the low-frequency infrared absorption strongly decreases at all frequencies with increasing salt concentration. It was also found that, in the concentration range from 0 to 12 M, the frequency dependence of the absorption could be well-described with a sum of two Debye relaxation modes with the same relaxation time constants as pure water.¹⁰⁵ This finding indicates that the ions have very little effect on the structural dynamics of the water molecules outside the first solvation shells.

4.4. Transient Vibrational Absorption Spectroscopy

The hydrogen-bond dynamics of water molecules outside the first anionic hydration shell have been studied with

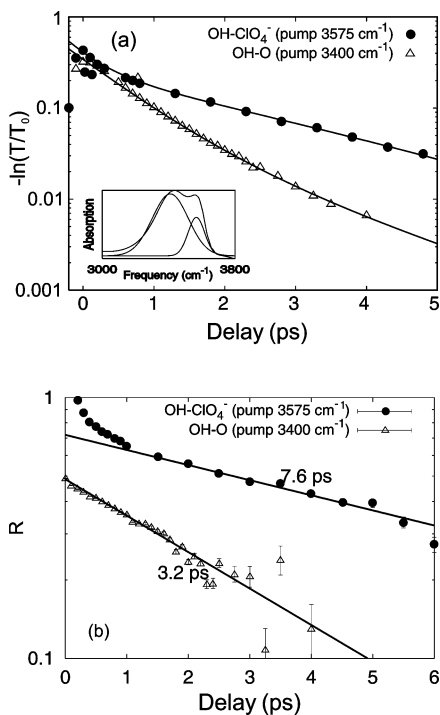


Figure 16. (a) Isotropic and (b) anisotropic signal measured for a solution of 6 M NaClO₄ in HDO/D₂O with two different combinations of pump and probe frequencies. The absorption spectrum is shown in the inset of (a). Reprinted with permission from ref 60. Copyright 2003 American Institute of Physics.

transient vibrational absorption spectroscopy using aqueous salt solutions for which the water molecules solvating the anion are spectrally well-separated from the spectral response of the other water molecules. For instance, for solutions of the perchlorate ion (ClO₄⁻), the OH···ClO₄⁻ absorption band of the hydration shell of this anion is quite well-separated from the OH···O absorption band of the other water molecules, because the OH···ClO₄⁻ hydrogen bond is non-directional and relatively weak, with the O–H groups pointing to the centers of the edges of the ClO₄⁻ tetrahedron.¹⁰⁶

In the inset of Figure 16, the absorption spectrum of the O–H stretch vibration of solutions of 6 M NaClO₄ in HDO/D₂O solution is shown. The spectrum is composed of two peaks: the peak centered at 3400 cm⁻¹ represents O–H groups hydrogen bonded to D₂O molecules, and the peak at 3575 cm⁻¹ represents O–H groups hydrogen bonded to the ClO₄⁻ ion.⁷ The HDO molecules bonded to D₂O molecules represent both bulk HDO molecules and HDO molecules in the solvation shell of the cation. The decay of the isotropic pump–probe signal is shown in Figure 16a. When pumping at 3575 cm⁻¹ (0 → 1 transition) and probing at 3325 cm⁻¹ (1 → 2 transition), the observed decay is biexponential. The fast component with a time constant of 0.8 ± 0.1 ps results from O–H groups that are hydrogen bonded to D₂O, and the slow component with a time constant of 2.2 ± 0.2 ps results from O–H groups bonded to the ClO₄⁻ anion. When the absorption band is pumped at 3400 cm⁻¹ (0 → 1 transition) and probed at 3150 cm⁻¹ (1 → 2 transition), no anion-bonded OH groups are observed, and the decay is single exponential with a time constant of ~0.8 ps.

In Figure 16b, the measured anisotropy is shown. At a pump frequency of 3575 cm⁻¹ and a probe frequency of 3325

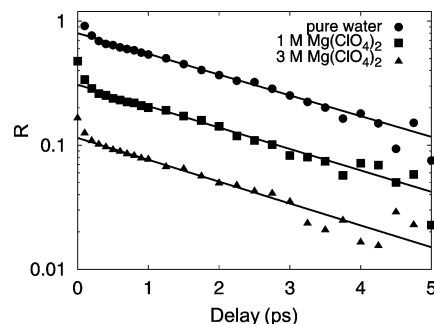


Figure 17. Anisotropy parameter R measured as a function of delay for solutions of different concentrations of Mg(ClO₄)₂ dissolved in HDO/H₂O. The pump and probe frequencies are 2500 cm⁻¹ and are resonant with the O–D vibration of the O–D···O groups. The data have been fitted with a single exponential and are shifted vertically with respect to each other for clarity. Reprinted with permission from ref 60. Copyright 2003 American Institute of Physics.

cm⁻¹, the signal is dominated by the orientational dynamics of the O–H···ClO₄⁻ groups. After 3 ps, the measured anisotropy only represents the orientational dynamics of these O–H groups, because of the difference in vibrational lifetime between the anion-bonded and the water-bonded O–H vibrations. The time constant of the orientational relaxation of the O–H···ClO₄⁻ groups is 7.6 ± 0.3 ps. At a pump frequency of 3400 cm⁻¹ and a probe frequency of 3150 cm⁻¹, the observed anisotropy decay is single exponential over the whole delay-time range and only represents the orientational relaxation of HDO molecules hydrogen bonded to D₂O molecules. This result shows that, for solutions containing ClO₄⁻, the orientational dynamics of the O–H···O hydrogen-bonded water molecules can indeed be studied without the measurements being affected by the contribution of anion-bonded water molecules.

To study the effect of the ions on the orientational dynamics of the bulk water molecules, the anisotropy dynamics were measured for solutions that contain ions that are believed to be strong structure makers, like Mg²⁺ and SO₄²⁻. The Jones–Dole B coefficients at room temperature of Mg(ClO₄)₂ and Na₂SO₄ solutions are 0.3 and 0.4, respectively.⁸² This means that the viscosity of 1 M Mg(ClO₄)₂ is ~30% higher than the viscosity of pure water, and the viscosity of 1 M Na₂SO₄ is even ~40% higher. By dissolving Mg(ClO₄)₂ in HDO/H₂O instead of HDO/D₂O, the orientational dynamics can be probed via the O–D stretch vibration. The vibrational relaxation time of the O–D stretch vibration of 1.7 ± 0.3 ps¹⁰⁷ is more than twice as long as the vibrational relaxation time of the O–H stretch vibration, which implies that the anisotropy decay can be followed over a much longer delay-time interval.

In Figure 17, the dynamics of R of solutions of Mg(ClO₄)₂ in HDO/H₂O are compared to the dynamics of R of pure HDO/H₂O. All solutions show the same anisotropy decay with a time constant of 2.5 ± 0.1 ps, which shows that the addition of Mg(ClO₄)₂ has a negligible effect on the orientational dynamics of the water-bonded water molecules. The same result was found for solutions containing SO₄²⁻ ions.⁶⁰ These results imply that ions do not affect the strength of the hydrogen-bond interactions *outside* the first hydration shell. The value of the orientational correlation time constant of 2.5 ± 0.1 ps agrees well with the value that was measured for pure liquid water with transient vibrational spectroscopy,⁵¹ NMR,^{49,50} and terahertz spectroscopy (taking into account a

factor of 3 between the relaxation time constants of the first and the second Legendre polynomial),^{103,104}

4.5. Molecular Dynamics Simulations

The long-range effects of ions on the hydrogen-bond structure of liquid water have also been studied theoretically using MD simulations. In all simulations, it is found that the hydrogen-bond structure of the first solvation shell strongly differs from that of liquid water and that, beyond this shell, the liquid rapidly acquires the structure of the pure liquid.^{18,84,108–112} In the second solvation shell of cations, the relative orientation of water molecules can be somewhat different from liquid water.^{18,84} In addition, it has been found in some simulations that the number of hydrogen bonds per water molecule can be slightly higher in the second shell of Na⁺ than in the bulk.^{108,110} However, in other MD simulations, this effect was not observed.^{109,111} For the Mg²⁺ ion, which is considered to be a strong structure maker, some studies found that the oxygen–oxygen distances between the first and the second solvation shell are shorter than in bulk liquid water, indicative of a strengthening of the hydrogen bonds.^{113,114} However, in a more recent study, the distance between the first and the second solvation shell was not found to be significantly smaller than the distance between water molecules in the pure liquid,¹¹² thus suggesting that even Mg²⁺ with its high charge density has a negligible long-range effect on the strength of the hydrogen bonds.

4.6. Discussion and Concluding Remarks

Most experimental techniques do not show a significant change of the hydrogen-bond structure of water outside the first solvation shell of the ions. In transient vibrational absorption spectroscopy, it was found that the orientational dynamics outside the first solvation shell are the same as in pure liquid water, even for solutions containing ions that are believed to be strong structure makers. In dielectric relaxation studies, the orientational dynamics were observed to become slightly faster when ions are added,⁷³ whereas low-frequency Raman and time-resolved Kerr effect studies show a slight slowing down of the dynamics. Here, it should be noted that the relaxation time constants measured in low-frequency Raman spectroscopy (~1 ps) are significantly shorter than the time scales for molecular reorientation deduced from transient vibrational absorption spectroscopy, NMR, and dielectric relaxation studies (4–8 ps). Hence, low-frequency Raman spectroscopy and optical Kerr effect studies appear to probe relaxation processes of the liquid that are different from the processes observed with the other techniques. Finally, molecular dynamics simulations show that ions can affect the orientation and density of hydrogen bonds beyond the first solvation shell, but the effects are small and rapidly vanish with increasing distance with respect to the ion.

It can be concluded that ions have a very limited effect on the hydrogen-bonded structure of liquid water outside the first solvation shell. This finding implies that the macroscopic properties of salt solutions, which were believed to be indicative of structure making or breaking, have to be explained from different effects. For instance, the effect of ions on the linear absorption spectrum must predominantly result from the influence of the ions on the structure and dynamics of the hydrogen bonds of the first hydration shell. Another important effect that was believed to be indicative of structure making/breaking is the effect of ions on the

viscosity of liquid water. In fact, the increase in viscosity is considered to be one of the prime indications for the structure-making effect on liquid water of ions like Mg²⁺. However, it should be realized that the viscosity is a macroscopic property that represents the average behavior of a large number of water molecules. This average behavior is clearly only a good measure for the behavior of the individual molecules if all molecules would show the same dynamics. The findings in section 2 and in this section show that the effects of ions on the orientational and translational dynamics of water are, in fact, extremely inhomogeneous. Transient vibrational absorption spectroscopy and molecular dynamics simulations show the translational dynamics of the water molecules in the first hydration shell to be 1 order of magnitude slower than the corresponding dynamics of pure liquid water. In contrast, beyond this shell, there is no measurable difference with pure liquid water. This means that an aqueous salt solution should not be viewed as a homogeneous liquid with a modified, uniform intermolecular interaction but rather as a colloidal suspension of more-or-less inert particles in pure liquid water, with the particles formed by the ions and their first hydration shells. In this picture, the viscosity at low concentration can be described by the Einstein equation,¹¹⁵

$$\frac{\eta - \eta_0}{\eta_0} \approx 2.5\phi$$

with ϕ being the volume fraction of the spheres.

It follows from this equation that a 30% increase of the viscosity, as observed for a 1 M Mg(ClO₄)₂ solution, can be obtained with a solution of 3 M suspended spheres that have a radius of ~250 pm. This colloidal radius compares quite well with the typical radius of an ion and its first hydration shell of water molecules. From the Einstein relation, it follows that a smaller increase in viscosity corresponds to a smaller colloidal radius. For instance, an increase in viscosity of 10%, as observed for a 1 M NaCl solution, corresponds to an average colloidal radius of the Na⁺ and Cl⁻ ions of only 200 pm. Here, it should be realized that the colloidal radius is determined not only by the radius of the ion and its first solvation shell but also by the residence time of the water molecules in this shell. With decreasing residence time, the effective colloidal radius will become smaller, and the increase in viscosity will be less. It is indeed found in molecular dynamics simulations that ions that strongly increase the viscosity (and that are believed to be structure makers) show much longer residence times for the water molecules in their hydration shells than ions that only weakly affect the viscosity (and that are believed to be structure breakers).²⁰ Hence, the large influence of some ions on the viscosity of water is not their ability to enhance the bulk hydrogen bond network but rather the rigidity (long lifetime) of their first hydration shells.

An interesting question is whether the above conclusions on the limited range of influence of ions on the structure of water also apply to more complex ionic systems showing multiple hydrogen-bond donor and acceptor sites like peptides and DNA molecules. Clearly, further research will be needed to provide the answer to this question. A recent study of the dynamics of water near the ionic surface of AOT (sodium bis(2-ethylhexyl)sulfosuccinate) reverse micelles showed that the first layer of water interacting with the ionic SO₃⁻ head groups at the surface is strongly immobilized.

Beyond this layer, the dynamics are not very different from those of bulk liquid water.¹¹⁶ Hence, also for this complicated ionic surface, the range over which the structural dynamics of the water is influenced by the ion appears to be limited to the first hydration shell.

5. Acknowledgments

Financial support from the “Stichting voor Fundamenteel Onderzoek der Materie (FOM)” and The Netherlands Research Council for Chemical Sciences (NWO–CW) is gratefully acknowledged.

6. References

- Waldron, R. D. *J. Chem. Phys.* **1957**, *26*, 809.
- Walrafen, G. E. *J. Chem. Phys.* **1962**, *36*, 1035.
- Terpstra, P.; Combes, D.; Zwick, A. *J. Chem. Phys.* **1990**, *92*, 65.
- Ohtaki, H.; Radnai, T. *Chem. Rev.* **1993**, *93*, 1157.
- Cox, W. M.; Wolfenden, J. H. *Proc. R. Soc., Ser. A* **1934**, *145*, 486.
- Gurney, R. W. *Ionic processes in solution*; McGraw-Hill: New York, 1953.
- Franks, F. *Water: a comprehensive treatise, Vol. 3*; Plenum Press: London, 1973.
- Impey, R. W.; Madden, P. A.; McDonald, R. *J. Phys. Chem.* **1983**, *87*, 5071.
- Sprick, M.; Klein, M. L.; Watanabe, K. *J. Phys. Chem.* **1990**, *94*, 6483.
- Dang, L. X.; Garret, B. C. *J. Chem. Phys.* **1993**, *99*, 2972.
- Dang, L. X.; Garret, B. C. *J. Chem. Phys.* **1993**, *99*, 6950.
- Smith, D. E.; Dang, L. X. *J. Chem. Phys.* **1994**, *100*, 3757.
- Tunon, I.; Martins-Costa, M. T. C.; Millot, C.; Ruiz-Lopez, M. F. *Chem. Phys. Lett.* **1995**, *241*, 450.
- Lyubartsev, A. P.; Laaksonen, A. *J. Phys. Chem.* **1996**, *100*, 16410.
- Stuart, S. J.; Berne, B. J. *J. Phys. Chem.* **1996**, *100*, 11934.
- Lee, S. H.; Rasaiah, J. C. *J. Phys. Chem.* **1996**, *100*, 1420.
- Tongraar, A.; Liedl, K. R.; Rode, B. M. *J. Phys. Chem. A* **1997**, *101*, 6299.
- Tongraar, A.; Liedl, K. R.; Rode, B. M. *J. Phys. Chem. A* **1998**, *102*, 10340.
- Hermansson, K.; Wojcik, M. *J. Phys. Chem. B* **1998**, *102*, 6089.
- Koneshan, S.; Rasaiah, J. C.; Lynden-Bell, R. M.; Lee, S. H. *J. Phys. Chem. B* **1998**, *102*, 4193.
- Tobias, D. J.; Jungwirth, P.; Parrinello, M. *J. Chem. Phys.* **2001**, *114*, 7036.
- Raugei, S.; Klein, M. L. *J. Chem. Phys.* **2002**, *116*, 196.
- Heuft, J. M.; Meijer, E. J. *J. Chem. Phys.* **2003**, *119*, 11788.
- Heuft, J. M.; Meijer, E. J. *J. Chem. Phys.* **2005**, *123*, 094506.
- Heilweil, E. J.; Doany, F. E.; Moore, R.; Hochstrasser, R. M. *J. Chem. Phys.* **1982**, *76*, 5632.
- Jimenez, R.; Fleming, G. R.; Kumar, P. V.; Maroncelli, M. *Nature* **1994**, *369*, 471.
- Pshenichnikov, M. S.; Duppen, K.; Wiersma, D. A. *Phys. Rev. Lett.* **1995**, *74*, 674.
- Hamm, P.; Lim, M.; Hochstrasser, R. M. *J. Chem. Phys.* **1997**, *107*, 10523.
- Hamm, P.; Lim, M.; Hochstrasser, R. M. *Phys. Rev. Lett.* **1998**, *61*, 5326.
- Zhong, Q.; Baronavski, A. P.; Owrutsky, J. C. *J. Chem. Phys.* **2003**, *118*, 7074.
- Zhong, Q.; Baronavski, A. P.; Owrutsky, J. C. *J. Chem. Phys.* **2003**, *119*, 9171.
- Woutersen, S.; Emmerichs, U.; Bakker, H. J. *Science* **1997**, *278*, 658.
- Laenen, R.; Rauscher, C.; Laubereau, A. *Phys. Rev. Lett.* **1998**, *80*, 2622.
- Woutersen, S.; Emmerichs, U.; Nienhuys, H. K.; Bakker, H. J. *Phys. Rev. Lett.* **1998**, *81*, 1106.
- Gale, G. M.; Gallot, G.; Hache, F.; Lascoux, N.; Bratos, S.; Leicknam, J.-C. *Phys. Rev. Lett.* **1999**, *82*, 1068.
- Woutersen, S.; Bakker, H. J. *Phys. Rev. Lett.* **1999**, *83*, 2077.
- Woutersen, S.; Bakker, H. J. *Nature* **1999**, *402*, 507.
- Deák, J. C.; Rhea, S. T.; Iwaki, L. K.; Dlott, D. D. *J. Phys. Chem. A* **2000**, *104*, 4866.
- Lock, A. J.; Woutersen, S.; Bakker, H. J. *J. Phys. Chem. A* **2001**, *105*, 1238.
- Fecko, C. J.; Eaves, J. D.; Loparo, J. J.; Tokmakoff, A.; Geissler, P. L. *Science* **2003**, *301*, 1698.
- Nibbering, E. T. J.; Elsaesser, T. *Chem. Rev.* **2004**, *104*, 1887.
- Deak, J. C.; Pang, Y.; Sechler, T. D.; Wang, Z.; Dlott, D. D. *Science* **2004**, *306*, 473.
- Steinel, T.; Asbury, J. B.; Zheng, J.; Fayer, M. D. *J. Phys. Chem. A* **2004**, *108*, 10957.
- Cowan, M. L.; Bruner, B. D.; Huse, N.; Dwyer, J. R.; Chugh, B.; Nibbering, E. T. J.; Elsaesser, T.; Miller, R. J. D. *Nature* **2005**, *434*, 199.
- Hunt, J. P.; Friedman, H. L. *Prog. Inorg. Chem.* **1983**, *30*, 359.
- Braun, B. M.; Weingärtner, H. *J. Phys. Chem.* **1988**, *92*, 1342.
- Hertz, H. G. In *The Chemical Physics of Solvation, Part B, Spectroscopy of Solvation*; Dogonadze, R. R., Kálmán, E., Kornyshev, A. A., Ulstrup, J., Eds.; Elsevier: Amsterdam, The Netherlands, 1987.
- Sacco, A. *Chem. Soc. Rev.* **1994**, *23*, 129.
- Smith, D. W. G.; Powles, J. G. *Mol. Phys.* **1966**, *10*, 451.
- Hindman, J. C.; Svirnickas, A.; Wood, M. J. *Chem. Phys.* **1974**, *59*, 1517.
- Nienhuys, H. K.; van Santen, R. A.; Bakker, H. J. *J. Chem. Phys.* **2000**, *112*, 8487.
- Tao, N. J.; Lindsay, S. M. *J. Phys. Cond. Matter* **1989**, *1*, 8709.
- Kropman, M. F.; Bakker, H. J. *Science* **2001**, *291*, 2118.
- Kropman, M. F.; Bakker, H. J. *J. Chem. Phys.* **2001**, *115*, 8942.
- Laenen, R.; Thaller, A. *Chem. Phys. Lett.* **2001**, *349*, 442.
- Kropman, M. F.; Nienhuys, H.-K.; Bakker, H. J. *Phys. Rev. Lett.* **2002**, *88*, 77601.
- Kropman, M. F.; Bakker, H. J. *Chem. Phys. Lett.* **2002**, *362*, 349.
- Kropman, M. F.; Bakker, H. J. *Chem. Phys. Lett.* **2003**, *370*, 741.
- Omta, A. W.; Kropman, M. F.; Woutersen, S.; Bakker, H. J. *Science* **2003**, *273*, 347.
- Omta, A. W.; Kropman, M. F.; Woutersen, S.; Bakker, H. J. *J. Chem. Phys.* **2003**, *119*, 12457.
- Kropman, M. F.; Bakker, H. J. *J. Am. Chem. Soc.* **2004**, *126*, 9135.
- Bergström, P.-A.; Lindgren, J. *J. Phys. Chem.* **1991**, *95*, 8575.
- Novak, A. *Struct. Bonding (Berlin)* **1974**, *18*, 177.
- Mikenda, W. *J. Mol. Struct.* **1986**, *147*, 1.
- Mikenda, W.; Steinböck, S. *J. Mol. Struct.* **1996**, *384*, 159.
- Rey, R.; Moller, K. B.; Hynes, J. T. *J. Phys. Chem. A* **2002**, *106*, 11993.
- Lawrence, C. P.; Skinner, J. L. *J. Chem. Phys.* **2003**, *118*, 264.
- Wójcik, M. J.; Lindgren, J.; Tegenfeldt, J. *Chem. Phys. Lett.* **1983**, *99*, 112.
- Graener, H.; Seifert, G.; Laubereau, A. *Chem. Phys. Lett.* **1990**, *172*, 435.
- Laage, D.; Hynes, J. T. *Proc. Natl. Acad. Sci. U.S.A.* **2007**, *104*, 11167.
- Out, D. J. P.; Los, J. M. *J. Chem. Soc.* **1980**, *9*, 19.
- Atkins, P. W. *Physical Chemistry*; Oxford University Press: Oxford, U.K., 1990.
- Wachter, W.; Kunz, W.; Buchner, R.; Hefter, G. *J. Phys. Chem. A* **2005**, *109*, 8675.
- Lock, A. J.; Bakker, H. J. *J. Chem. Phys.* **2002**, *117*, 1708.
- Nienhuys, H. K.; Woutersen, S.; van Santen, R. A.; Bakker, H. J. *J. Chem. Phys.* **1999**, *111* (4), 1494.
- Hashimoto, K.; Morokuma, K. *Chem. Phys. Lett.* **1994**, *223*, 423.
- Asada, T.; Nishimoto, K. *Chem. Phys. Lett.* **1995**, *232*, 518.
- Ramaniah, L. M.; Bernasconi, M.; Parrinello, M. *J. Chem. Phys.* **1998**, *109*, 6839.
- Staub, A.; Hynes, J. T. *Chem. Phys. Lett.* **1993**, *204*, 197.
- Ayotte, P.; Weddle, G. H.; Kim, J.; Johnson, M. A. *J. Am. Chem. Soc.* **1998**, *120*, 12361.
- Nitzan, A.; Jortner, J. *J. Mol. Phys.* **1973**, *25*, 713.
- Marcus, Y. *Ion Solvation*; John Wiley & Sons: Chichester, U.K., 1985.
- Rempe, S. B.; Pratt, L. R. *Fluid Phase Equilib.* **2001**, *183*, 121.
- Zhu, S.-B.; Robinson, G. W. *J. Chem. Phys.* **1992**, *97*, 4336.
- Buchner, R.; Hefter, G. T.; May, P. M. *J. Phys. Chem. A* **1999**, *103*, 1.
- Buchner, R.; Hefter, G. T.; May, P. M.; Sipos, P. *J. Phys. Chem. B* **1999**, *103*, 11186.
- Lawrence, C. P.; Skinner, J. L. *J. Chem. Phys.* **2003**, *119*, 3840.
- Jones, G.; Dole, M. *J. Am. Chem. Soc.* **1929**, *51*, 2950.
- Falkenhagen, H.; Dole, M. *Phys. Z.* **1929**, *30*, 611.
- Zwanzig, R. *J. Chem. Phys.* **1963**, *38*, 1603.
- Wang, Y.; Tominaga, Y. *J. Chem. Phys.* **1994**, *101*, 3453.
- Mizoguchi, K.; Ujike, T.; Tominaga, Y. *J. Chem. Phys.* **1998**, *109*, 1867.
- Amo, Y.; Tominaga, Y. *Phys. Rev. E* **1998**, *58*, 7553.
- Ujike, T.; Tominaga, Y.; Mizoguchi, K. *J. Chem. Phys.* **1999**, *110*, 1558.
- Foggi, P.; Bellini, M.; Kien, D. P.; Verucque, I.; Righini, R. *J. Phys. Chem. A* **1997**, *101*, 7029.
- Kaatze, U. *J. Phys. Chem.* **1987**, *91*, 3111.
- Nörtemann, K.; Hilland, J.; Kaatze, U. *J. Phys. Chem. A* **1997**, *101*, 6864.
- Hubbard, J. B.; Onsager, L. *J. Chem. Phys.* **1977**, *67*, 4850.
- Barthel, J.; Schmithals, F.; Behret, H. Z. *Phys. Chem. NF* **1970**, *71*, 115.

- (100) Filimonova, Z. A.; Lileev, A. S.; Lyashchenko, A. K. *Russ. J. Inorg. Chem.* **2002**, *47*, 1890.
- (101) Kaatze, U. *Ber. Bunsen-Ges. Phys. Chem.* **1973**, *77*, 447.
- (102) Barthel, J.; Krüger, J.; Schollmeyer, E. *Z. Phys. Chem. NF* **1977**, *104*, 59.
- (103) Kindt, J. T.; Schutzenmaier, C. A. *J. Phys. Chem.* **1996**, *100*, 10373.
- (104) Rønne, C.; Thrane, C.; Åstrand, P.-O.; Wallqvist, A.; Keiding, S. R. *J. Chem. Phys.* **1997**, *107*, 5319.
- (105) Dodo, T.; Sugawa, M.; Nonaka, E. *J. Chem. Phys.* **1993**, *98*, 5310.
- (106) Walrafen, G. E. *J. Chem. Phys.* **1970**, *52*, 4176.
- (107) Kropman, M. F.; Nienhuys, H. K.; Woutersen, S.; Bakker, H. J. *J. Phys. Chem. A* **2001**, *105*, 4622.
- (108) Chandrasekhar, J.; Jorgensen, W. L. *J. Chem. Phys.* **1982**, *77*, 5080.
- (109) Chandrasekhar, J.; Spellmeier, D. C.; Jorgensen, W. L. *J. Am. Chem. Soc.* **1984**, *106*, 903.
- (110) Obst, S.; Bradaczek, H. *J. Phys. Chem.* **1996**, *100*, 15677.
- (111) White, J. A.; Schwegler, E.; Galli, G.; Gygi, F. *J. Chem. Phys.* **2000**, *113*, 4668.
- (112) Lightstone, F. C.; Schwegler, E.; Hood, R. Q.; Gygi, F.; Galli, G. *Chem. Phys. Lett.* **2001**, *343*, 549.
- (113) Palinkas, G.; Radnai, T.; Dietz, W.; Szasz, G. I.; Heinzinger, K. *Z. Naturforsch.* **1982**, *37A*, 1049.
- (114) Mayer, I.; Lukovits, I.; Radnai, T. *Chem. Phys. Lett.* **1992**, *188*, 595.
- (115) Einstein, A.; Furth, A.; Cowper, A. D. *Investigations on the theory of Brownian movement*; Dover: New York, 1926.
- (116) Doktor, A. M.; Woutersen, S.; Bakker, H. J. *Proc. Natl. Acad. Sci. U.S.A.* **2006**, *103*, 15355.

CR0206622